ECMWF

European Centre for Medium-Range Weather Forecasts

Newsletter

No. 169 | Autumn 2021

Extreme rain in Germany and Belgium

IFS upgrade

Assimilating Spire and COSMIC-2 data

Advanced regridding in Metview

European Centre for Medium-Range Weather Forecasts, Shinfield Park, Reading, RG2 9AX, UK

Publication policy

The ECMWF Newsletter is published quarterly. Its purpose is to make users of ECMWF products, collaborators with ECMWF and the wider meteorological community aware of new developments at ECMWF and the use that can be made of ECMWF products. Most articles are prepared by staff at ECMWF, but articles are also welcome from people working elsewhere, especially those from Member States and Co-operating States.

The ECMWF Newsletter is not peer-reviewed.

Any queries about the content or distribution of the ECMWF Newsletter should be sent to Georg.Lentze@ecmwf.int

Guidance about submitting an article and the option to subscribe to email alerts for new Newsletters are available at *www.ecmwf.int/en/about/media-centre/media-resources*

A look to the future

Earlier this month, ECMWF delivered the second upgrade of the Integrated Forecasting System (IFS) this year, to IFS Cycle 47r3. The upgrade includes a range of developments in the model and the use of observations, notably an enhanced usage of satellite data in cloudy regions. It brings some clear improvements to forecasts: it improves the large-scale atmospheric circulation and overall precipitation scores, and it reduces tropical cyclone track errors. But its main significance lies in a reworking of the moist physics to prepare for future resolution upgrades. This has been a major piece of work. It has involved ensuring that the complicated interactions between turbulence in the lowest part of the atmosphere, convective motions and cloud physics are described as scale-independently as possible. These developments make it possible for the IFS to be run across a broader range of horizontal resolutions, including convection-permitting resolutions. It has been shown that the new moist physics works better than the previous one on grid spacings of 3–5 km. Its implementation is thus a necessary step towards refining the horizontal resolution of the IFS, which currently uses grid spacings of 9 km for high-resolution forecasts and 18 km for ensemble forecasts.

Why do we need to aim for greater horizontal resolution? First, experience shows that it brings improvements in forecast performance in its own right. This is certainly true if the increase in resolution goes hand in hand with a careful reworking of the physics of the model. Second, our forecasts will be even better also as boundary conditions for limited-area models (LAMs) in operation in our Member and Co-operating States and for a wide range of other applications. The first horizontal resolution upgrade since 2016 is planned for next year. Watch this space!

This Newsletter provides interesting glimpses of other aspects of the future. One article notes that ECMWF now runs a three-site operation, in Reading (UK), Bologna (Italy) and Bonn (Germany). This will in particular allow the two EU Copernicus Earth observation services we operate to thrive after the UK left the EU. Other pieces are about new ways of supporting users of ECMWF forecasts and of our Copernicus websites; an update on our use of radiosonde descent data; and our participation in a forward-looking project to develop a new generation of Earth system models. One feature article describes the positive effects of a forthcoming greater use of Global Navigation Satellite System Radio Occultation data to help determine the initial conditions of forecasts; another explores how users can post-process forecast results beyond the default behaviour using new functionalities.

What all these developments show is that we must never forget to look to the future when we strive to optimise our forecasts and services for our users. It is the only way to remain on top of our key tasks.

Florence Rabier
Director-General

Contents

Editorial
A look to the future 1

News
Extreme rain in Germany and Belgium in July 2021 2
Drifting buoys deployed off Greenland 4
Use of radiosonde descent data from ships 5
Retrospective two-year ENSO predictions during the 20th century 6
Newsletter questionnaire 7
ECMWF supports Croatian met service during data centre move 8
ECMWF Support Portal – for all users and queries 9
The Climate Data Store Virtual Assistant 10
2022 Training Courses: registrations close soon 11
Working on tropical cyclone predictions at ECMWF 12
ECMWF becomes a multi-site organisation 13
ECMWF Summer of Weather Code drives open-source developments and innovation 14
ECMWF helps EUCOS to monitor observations 15
ECMWF contributes to new Earth system models 16
New observations since July 2021 16

Meteorology
IFS upgrade improves moist physics and use of satellite observations 17
Assimilating Spire and COSMIC-2 data into the IFS 25

Computing
Advanced regridding in Metview 33

General
ECMWF publications 37
ECMWF Calendar 2021/22 37
Contact information 38

Editor Georg Lentze • **Typesetting & Graphics** Anabel Bowen • **Cover** See the prediction figure on page 3

Extreme rain in Germany and Belgium in July 2021

Linus Magnusson, Adrian Simmons, Shaun Harrigan, Florian Pappenberger

On 14 July, parts of western Germany, north-eastern France, eastern Belgium, the eastern Netherlands and Luxembourg were hit by extreme rainfall leading to devastating flooding in small and medium-sized rivers, such as the Meuse and Ahr. The event caused more than 200 fatalities in Germany and Belgium. In this article, we discuss (i) how extreme the event was in the ERA5 reanalysis from the Copernicus Climate Change Service (C3S) and (ii) predictions of the event in ECMWF precipitation forecasts. However, rainfall predictions are only a part of the forecast value chain, which reaches from observations and numerical weather forecasts, via hazard and impact modelling, to public warnings and ultimately actions, and there are many aspects not covered here.

Meteorological background

The event was connected to an upper-level trough that caused extreme weather from the UK to Romania during its propagation from the Atlantic to south-eastern Europe. In the days leading up to the event, Switzerland, south-western Germany and eastern France also saw heavy precipitation. From 13 July to the early morning of 15 July, exceptional rainfall occurred on the north-western side of the cut-off low, in the warm and moist air stream from the north-east. This led to extreme amounts of rain on the eastern side of the low mountain ranges on the border between Germany and Belgium. Several stations on the German side measured more than 150 mm/48 h. In eastern Belgium the observation coverage is sparse in the ECMWF verification system, but according to the Royal Meteorological Institute of Belgium the town of Jalhay received 271 mm and Spa 217 mm over the same period.

Rainfall

For the evaluation, we focus on rainfall from 13 July 06 UTC to 15 July 06 UTC in a box (50–51°N, 5.5–7°E) covering the eastern part of Belgium and the worst-affected region in Germany, and also small parts of the Netherlands and Luxembourg (see the ERA5 precipitation map). The first question to ask is how extreme this event was in a historical perspective. To answer this, we make use of nearly 72 years of ERA5 precipitation data as a proxy for observations. Precipitation totals for the box have been calculated for all 48-hour intervals since January 1950, with steps of one day. The 48-hour window starting at 06 UTC on 13 July 2021 has by far the heaviest precipitation, with 104 mm (see the ERA5 precipitation distribution chart). The value is almost twice what was previously the heaviest precipitation in the period since 1950 (excluding the overlapping 48-hour interval starting on 06 UTC on 14 July 2021).

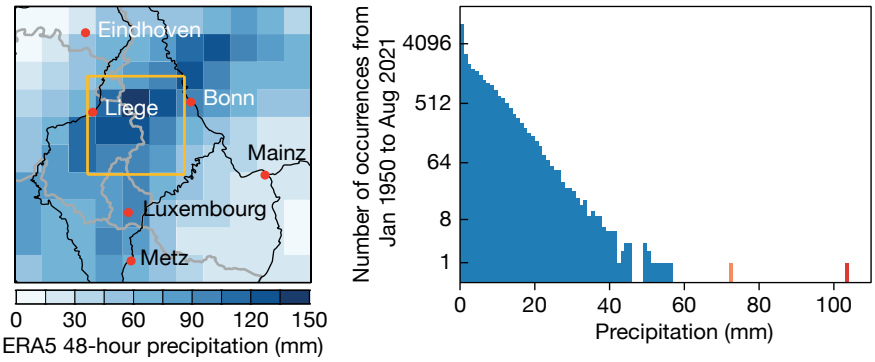

Precipitation record. The left-hand chart shows 48-hour precipitation from the ERA5 reanalysis for 13 July 06 UTC to 15 July 06 UTC. The yellow box highlights the area of 50–51°N and 5.5–7°E. The right-hand chart shows the distribution of 48-hour ERA5 precipitation for all days from January 1950 to August 2021 in that area. The period 13 July 06 UTC to 15 July 06 UTC 2021 is denoted by the red bar and 14 July 06 UTC to 16 July 06 UTC by the orange bar.

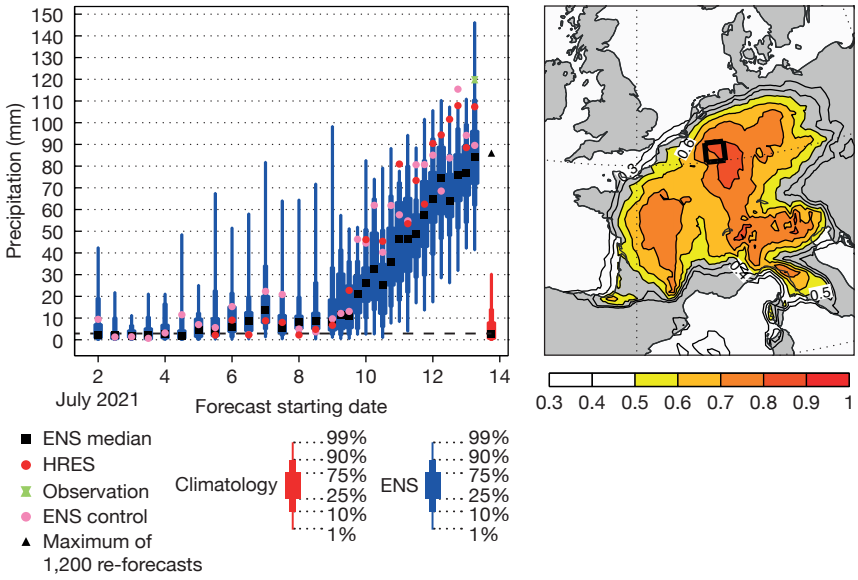

Rain forecasts and Extreme Forecast Index. The left-hand chart shows the evolution of forecasts for 48-hour precipitation from 13 to 15 July 06 UTC in the worst-affected region, indicated by the box in the right-hand plot. The average amount of precipitation recorded by weather stations is indicated as a green hourglass symbol. The right-hand chart shows the Extreme Forecast Index (EFI) for 3-day precipitation valid 13–15 July in a forecast from 10 July 00 UTC. The box highlights the same area as in the ERA5 chart.

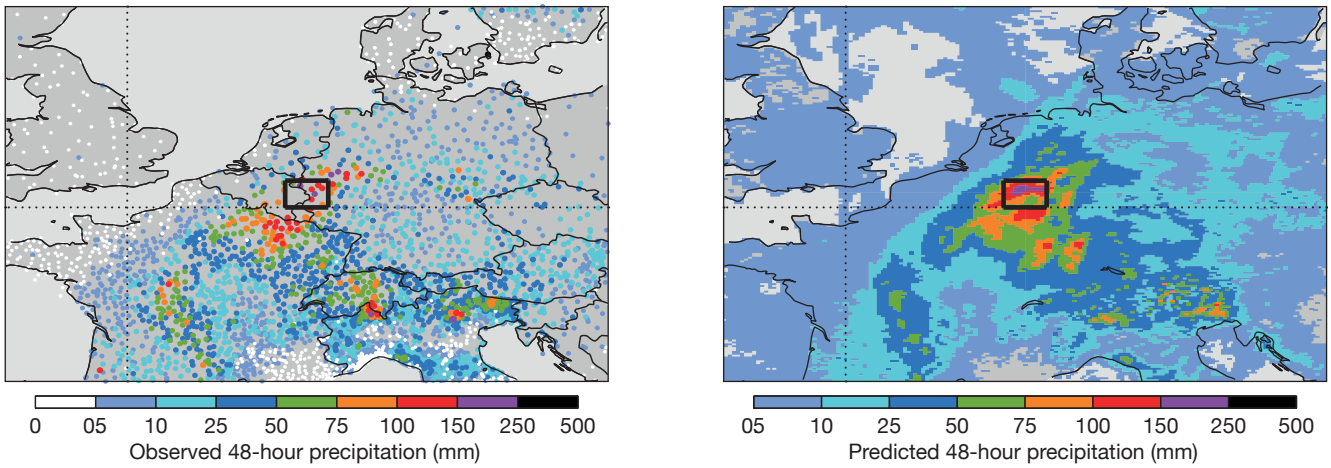

Observed rainfall and short-range forecast. The left-hand chart shows observations of 48-hour precipitation from 13 July 06 UTC to 15 July 06 UTC. The right-hand chart shows the corresponding HRES forecast from 13 July 06 UTC. The boxes highlight the same area as in the ERA5 chart.

Looking at the prediction of the event, the ensemble forecasts from 10 July for the same region started to pick up a signal of significantly wetter than normal conditions (see the box-and-whisker plot). At this time, the 3-day Extreme Forecast Index (EFI) gave a broad-scale signal over western Europe, with the strongest signal over western Germany (see the EFI chart). From 11 July 00 UTC onwards, the ensemble median was above the 99th percentile of the model climate for the 48-hour event discussed above. In the last ensemble forecast (ENS) before the event, the ensemble median was about the same as the maximum found in ECMWF's 1,200 re-forecasts based on day 5–7 forecasts over the past 20 years valid at the same time of year, and with much higher precipitation in some ensemble members. The predicted area-average precipitation in the last high-resolution forecast (HRES) before the event (107 mm) was somewhat lower than the average over the stations in the box (120 mm). However, looking at the observation map, with a gap in available observations for the worst-affected region in Belgium, it is likely the real area-average precipitation was higher, and it is therefore plausible that the ECMWF forecasts underestimated the quantity (see the observation map and short-range forecast for 48-hour precipitation).

Water absorption and runoff

The intense rainfall over steep valleys caused the most devastating and fastest developing flood waves, causing considerable destruction in towns such as Schuld, Altenahr and Dernau on the River Ahr, a small tributary of the Rhine. The complex terrain and local geology have been highlighted as contributing factors to the severity of the event.

The mountains in the region are quite low but relatively steep, and the soil on top of the bedrock is very thin, both factors leading to a rapid runoff into rivers. The local scale complexity challenges the soil model in terms of distributing the predicted precipitation between local storage and runoff into rivers and ground water. In the shortest HRES forecasts, the ECMWF Land Surface Modelling System (ECLand) in the Integrated Forecasting System (IFS) predicted up to 20–25% of the total rainfall in the box to directly go into runoff, while the rest of the water was absorbed by the soil locally. While this quantity is very hard to observe under these conditions, the prediction is likely to be an underestimation. Currently, separate soil models are used for numerical weather prediction (NWP) and flood forecasting purposes at ECMWF. Plans for kilometre-scale soil modelling in the IFS include making the model more suitable for predicting runoff by increasing the number of levels in the soil model and having a more integrated approach between NWP and hydrological forecasting. The long-term aim is to achieve a calibrated set of hydrological parameters that simultaneously improve evaporation into the atmosphere, long-term memory in the soil, and river discharge forecasts on both slow timescales, e.g affecting the fresh-water flux into oceans, and a fast timescale to predict flash-floods like the event described in this article.

Flood forecasts

The ECMWF HRES and ENS, together with forecasts from the German National Meteorological Service (DWD) and COSMO-LEPS (the Limited Area Ensemble Prediction System developed by the COSMO consortium), are used in the European Flood Awareness System (EFAS) of the Copernicus Emergency Management Service (CEMS).

The EFAS system provides forecasts for discharge in medium-sized and large rivers, and flash-flood forecasts for small rivers. ECMWF is the computational centre of EFAS, which issued flood forecasts for this event.

A detailed evaluation of the EFAS forecasts for this event is currently being undertaken in collaboration with other EFAS centres and the Joint Research Centre (JRC) of the European Commission, and will be presented at a later stage.

Conclusion

The magnitude of rainfall in the worst-affected region broke the record in the ERA5 reanalysis by a large margin. ECMWF forecasts predicted an extreme event with high confidence 3 days before the start of the 2-day event, but with large uncertainties about the absolute magnitude and how the rainfall would translate to runoff into rivers.

Drifting buoys deployed off Greenland

David Lavers (ECMWF), Eleanor Frajka-Williams (National Oceanography Centre, UK), Luca Centurioni, Anna Wilson, Marty Ralph (all Scripps Institution of Oceanography, US), Jacqueline Sugier (Met Office, UK)

In August and September 2021, 18 drifting buoys were deployed off southern Greenland and in the Davis Strait. An important feature of these buoys for ECMWF is that they provide valuable sea-level pressure observations in this region. Measurements of sea-level pressure are crucial for numerical weather prediction as (i) it is an important variable linked to the main mode of extratropical synoptic variability; (ii) many ocean areas have few other in-situ observations; and (iii) satellite data still only provide a small amount of information about pressure at mean sea level. The buoys can operate for up to two years and are a cost-effective component of the global observing system.

How the deployment came about

This deployment was made possible by a project entitled Targeted Experiment to Reconcile Increased Freshwater with Increased Convection (TERIFIC), which is funded under the European Union's Horizon 2020 research and innovation programme (grant agreement No. 803140). Within TERIFIC, drifting buoys are being deployed to understand the pathways by which the meltwaters from Greenland and the Arctic make their way to the open ocean, and in turn affect the large-scale ocean circulation. In this region – the Labrador Sea – ocean stratification is relatively weak, which means that wintertime storms and heat loss from the ocean to the atmosphere enables surface waters to mix down to depths of one kilometre or more in a process known as deep ocean convection. TERIFIC has set out to monitor this exchange and diagnose the processes controlling the rate and efficiency of freshwater export.

The drifting buoys to be launched in TERIFIC initially had no pressure sensors on board. However, a collaboration between ECMWF, the EUMETNET Surface Marine Programme (E-SURFMAR), the Lagrangian Drifter Laboratory and the Center for Western Weather and Water Extremes (CW3E) (the last two at Scripps Institution of Oceanography) enabled 17 of the 18 buoys to provide pressure observations. The Surface Velocity Program Barometer drifters (SVPB; https://gdp.ucsd.edu/ldl/svpb/) they use were funded by E-SURFMAR, the Global Drifter Program funded by the US National Oceanic and Atmospheric Administration (https://gdp.ucsd.edu/ldl/global-drifter-program/), the California Department of Water Resources, and the U.S. Army Corps of Engineers.

Potential for better forecasts

Two ships were used to release the buoys, a Woods Hole Oceanographic Institution ship off southern Greenland in August, and the USCGC Healy in the Davis Strait in September. The sea-level pressure observations from these extra buoys have been assimilated into the ECMWF Integrated Forecasting System since shortly after their release, providing forecast benefits across the northwest North Atlantic Ocean and the potential to improve forecast skill over Europe in the medium range. This deployment is also timely with the forthcoming winter season and storm activity.

Further information on pressure observations from drifting buoys is available in Ingleby and Isaksen (2018; doi.org/10.1002/asl.822), Centurioni et al. (2017; doi.org/10.1175/BAMS-D-15-00080.1), and Horányi et al. (2017; doi.org/10.1002/qj.2981).

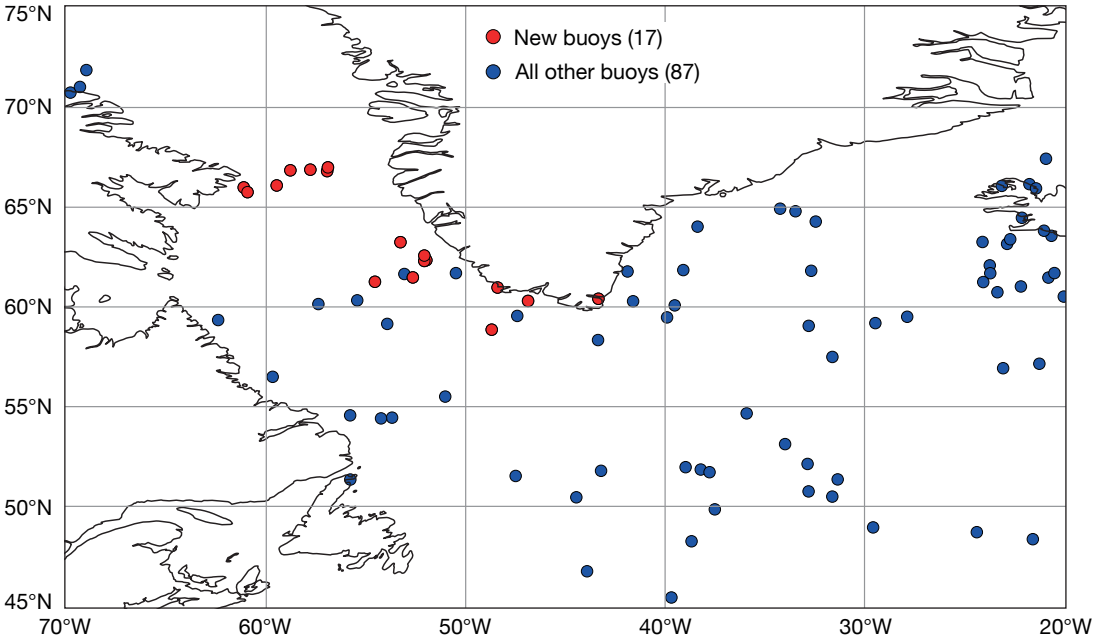

Drifting buoys in the northwest North Atlantic. The figure shows the location of all drifting buoys that reported pressure in the northwest North Atlantic Ocean on 22 September 2021. Red markers refer to the newly deployed drifting buoys. The number of buoys is given in the legend.

Use of radiosonde descent data from ships

Bruce Ingleby

In 2018, we reported that radiosonde descent data looked promising (ECMWF Newsletter No. 157). The data after balloon burst can provide an extra profile. Last year, ECMWF began to assimilate descent data from radiosondes launched in Germany, and recently it started to assimilate descent data from radiosondes launched from ships.

German radiosondes

In June 2020, following an assimilation experiment, ECMWF started assimilating descent data from Vaisala RS41 radiosondes launched in Germany. The German national meteorological service (DWD) also started using these data at a similar time. The data quality is best from radiosondes with a) a pressure sensor and b) a parachute – the German radiosondes have both. After balloon burst the radiosondes can fall very fast, up to 100 m/s or more, although the descent rate is very variable and reduced with a parachute. Whilst falling fast, the measured temperatures are too high, apparently due to frictional heating. As the air density increases, the descent rate slows. Without a pressure sensor, the temperature biases can cause an offset in the descent pressures in the troposphere. It is possible to use the descent rate to correct most of the error. When this is applied in the Vaisala processing, we expect to use descent data from more stations. Much more detail on these issues is available in a manuscript ('On the quality of RS41 radiosonde descent data') under open review at *Atmospheric Measurement Techniques*.

Ship-based radiosondes

In May 2021, a number of ships started reporting radiosonde descent data. Most of these are from the European Automated Shipboard Aerological Programme (ASAP) in the North Atlantic (see the map; for more details on ASAP, see ECMWF Newsletter No. 157). Four of these ships are using the RS41 radiosondes, and the descent quality looks good (see the graph). ECMWF started using the data operationally on 8 September 2021. Data use is restricted to pressures greater than 150 hPa, as for the land stations, to avoid very fast fall rates. These radiosondes have pressure sensors but not parachutes. They use smaller balloons than most land stations, and the temperature bias problems at upper levels are slightly less because they do not go as high. Five ships are providing descent data from Graw radiosondes; the quality makes the data unusable for now. Some ships use Modem radiosondes, but these are not providing descent data yet.

On average, radiosonde profiles from ships have more impact than land profiles because they are in data-sparse regions. At land stations, the descent reports often stop some kilometres above the surface due to hills blocking the radiosonde signal, but for ships the descent reports can get very close to the surface. We hope to have more usable descent reports from ship and land stations in the future.

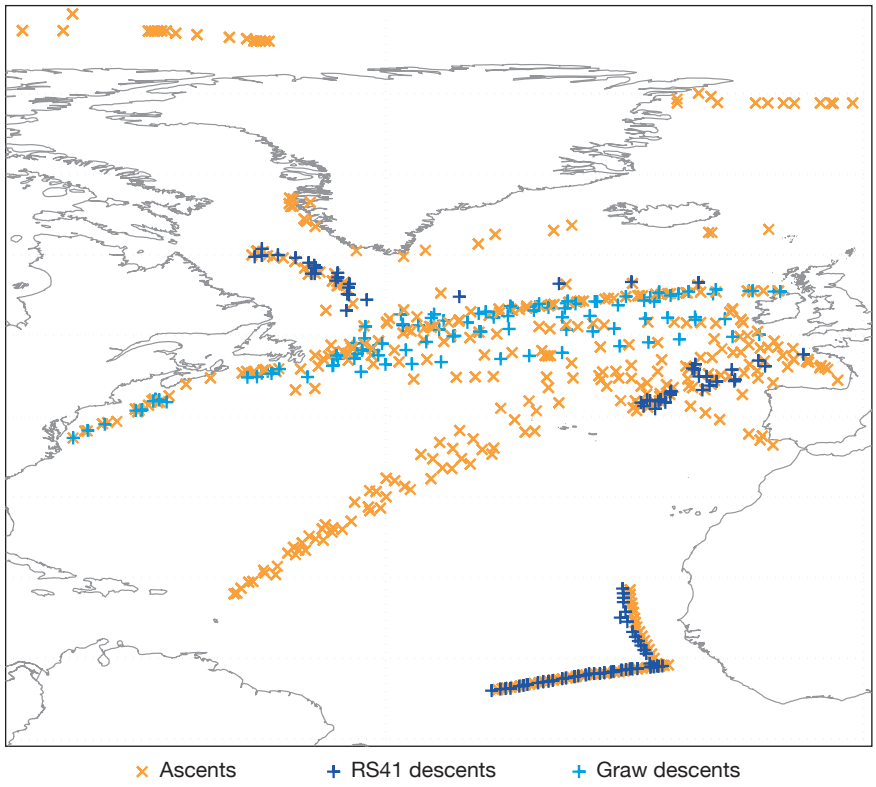

Radiosonde data in the North Atlantic. The map shows radiosonde data from ships in the North Atlantic in August 2021. The marks correspond to launch and balloon burst locations. The burst occurs usually 1.5 to 2 hours after launch. There are currently 17 ASAP ships, but typically only five or so are active on any given day. Some of the profiles are from research vessels (in the Arctic sea and in the tropics west of Africa in this figure).

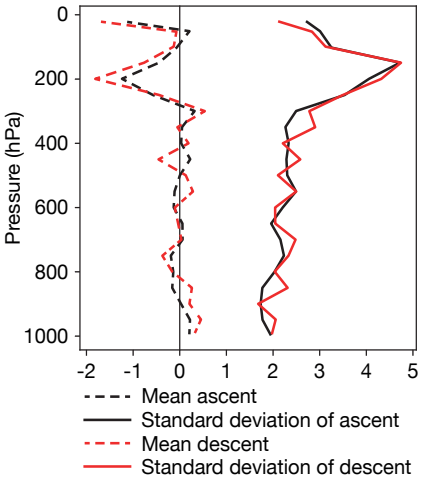

Fit of radiosonde winds to background winds. The chart shows the fit of radiosonde zonal (latitudinal) winds to interpolated ECMWF background winds. The radiosondes are from four ships providing RS41 descents for June to August 2021.

Retrospective two-year ENSO predictions during the 20th century

Antje Weisheimer, Magdalena Balmaseda, Tim Stockdale, Michael Mayer, Eric de Boisséson, Retish Senan, Stephanie Johnson

Large-scale fluctuations of the equatorial atmosphere and ocean over the tropical Pacific, known as El Niño–Southern Oscillation (ENSO), play an important role in the climate system. Forecasting ENSO is at the very heart of seasonal predictions because it provides the largest source of predictability on timescales of months and seasons ahead, and it is of great relevance to society.

A number of global teleconnections of ENSO link the variability over the tropical Pacific with remote regions of the world and contribute substantially to seasonal forecast skill in the extratropics of both hemispheres. Retrospective seasonal forecasts at ECMWF and other centres around the world cover the well-observed recent period from the 1980s onward and are essential to estimate and calibrate the skill of operational forecasts. Here we report about a new historical retrospective research forecasting dataset, created with a version of ECMWF's operational seasonal prediction system SEAS5, that covers all of the 20th century with forecast lead times of two years. The dataset, called SEAS5-20C, will be used to advance our understanding of the predictability of ENSO in the past and the future.

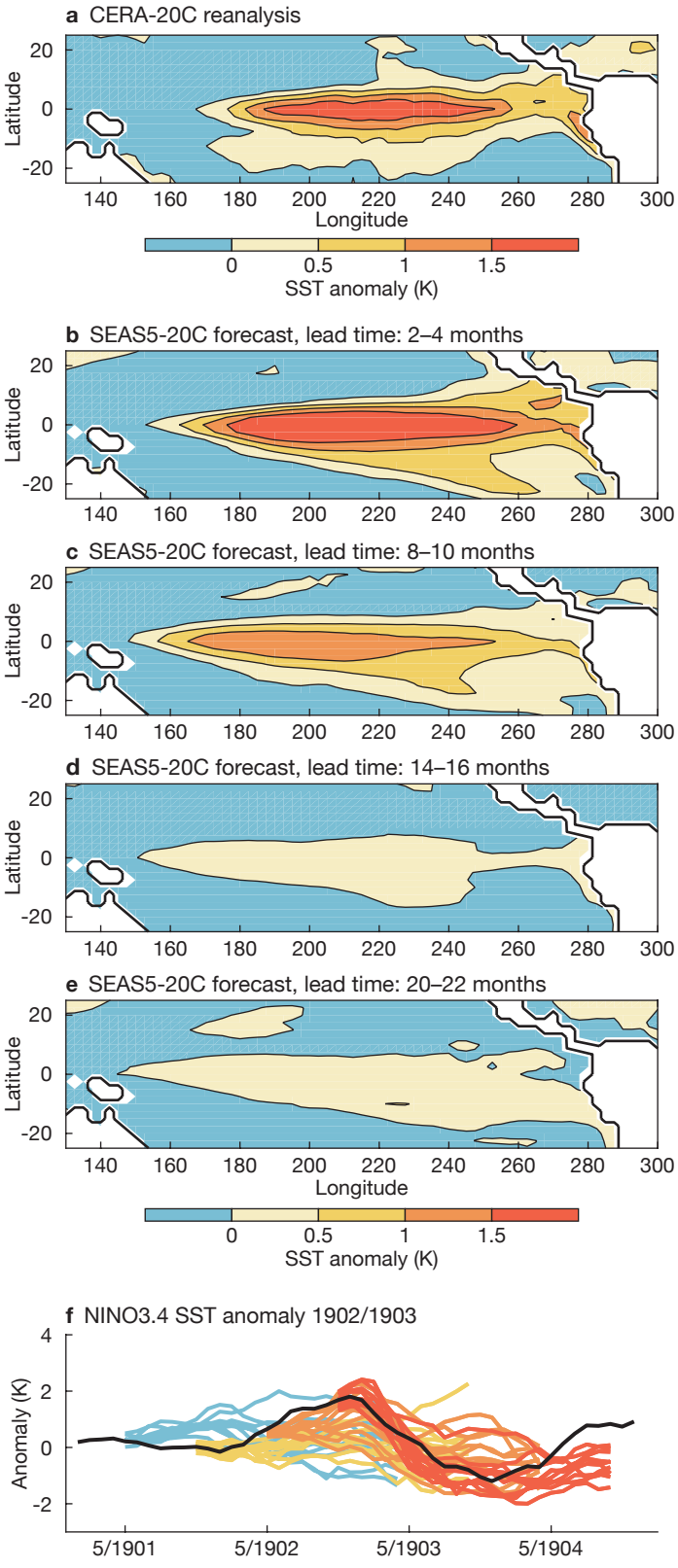

Retrospective forecasts of the 1902/1903 El Niño in SEAS5-20C. The top chart (a) shows the tropical Pacific SST anomaly during DJF in the reanalysis CERA-20C, while (b)–(e) show the ensemble mean SST anomaly during DJF in SEAS5-20C forecasts at different lead times: (b) initialisation in November 1902 and lead-time 2–4 months, (c) initialisation in May 1902 and lead-time 8–10 months, (d) initialisation in November 1901 and lead-time 14–16 months, (e) initialisation in May 1901 and lead-time 20–22 months. Panel (f) shows the NINO3.4 SST anomaly as plumes from all four start dates (in colour) and in CERA-20C (black).

ENSO re-forecasts

ENSO is an irregular coupled mode of variability that displays a diverse range of spatial structures, amplitudes and life cycles. The location of warm El Niño sea-surface temperature (SST) anomalies can be widely spread, from the Eastern to the central equatorial Pacific. Substantial non-monotonic variations in the amplitude of ENSO SST signals that are poorly understood have occurred during the 20th century. Nor do we understand very well the factors determining the occurrence and predictability of consecutive El Niño or La Niña years. With an average frequency of four to five years, there is only a very limited number of ENSO cases available in operational re-forecast records, and sampling the wide spectrum of ENSO flavours is not possible. In the presence of considerable variations in the coupled ocean–atmosphere system, good skill in predicting the most recent ENSO events cannot guarantee that future events will have similar predictability.

In order to further improve our confidence to predict future ENSO events and to explore potential ENSO skill beyond the seasonal timescale, we have performed a novel set of re-forecasts with a lead time of 24 months covering the extended 20th century period from 1901 to 2010. The simulations were done with a reduced-resolution version of ECMWF's operational seasonal system SEAS5 and comprise ensembles of 10 members for forecast start dates every May and November during the 110-year hindcast period. The initial states of the ocean, sea-ice, waves, atmosphere and land of the re-forecasts were taken from ECMWF's first coupled reanalysis of the 20th century, CERA-20C, which assimilated temperature and salinity in the ocean and sea-level pressure and marine wind data in the atmosphere.

As an example, the figure shows retrospective forecasts of the strong El Niño event that occurred in the December–January–February (DJF) season of 1902/03. CERA-20C (panel (a)) displays a large area of warm temperature anomalies with a maximum in the central equatorial Pacific. SEAS5-20C re-forecasts of this event show the DJF SST ensemble mean anomalies from the forecasts initialised 3 months (b), 9 months (c), 15 months (d) and 21 months ahead (e). We see that on seasonal timescales the El Niño event was well predicted. Even at the longest forecast range of 21 months (e), the forecast indicated a wide-spread yet weak warming across the central equatorial Pacific.

Panel (f) compiles the individual ensemble member realisations for the NINO3.4 SST index (area-averaged SSTs over the box 5°S–5°N and 120–170°W) anomaly from the four initialisation times of panels (b)–(e) that target the DJF 1902/03 season, with the black line showing the evolution of NINO3.4 SST anomalies in the verifying CERA-20C reanalysis. The forecast from November 1902 (red) follows the CERA-20C evolution of the peak warming and the subsequent cooling extremely well, with all ensemble members indicating positive SST anomalies during DJF. The May 1902 forecast (orange) has a 90% probability for DJF SST anomalies >0, while the forecasts from November 1901 (yellow) and May 1901 (blue) give an overall indication for likely positive SST anomalies during the peak season DJF (forecast probabilities of 60%).

Outlook

The re-forecasts show substantial decadal modulations of ENSO properties, and variable skill, which is the subject of ongoing investigations. Several sensitivity experiments that test the impact of sub-surface ocean observations and the role of atmospheric forcings at initial time have also been performed. SEAS5-20C is an important resource to study the complex predictability behaviour of ENSO, including multi-decadal skill variations and multi-year ENSO events. It will further be used to explore the feasibility of extending skilful ENSO predictions beyond one year. The DOI for the data discussed in this article is doi.org/10.21957/fzf9-te33.

Newsletter questionnaire

You are invited to take part in a short questionnaire on the ECMWF Newsletter to improve and develop it further.

To access it, please visit the questionnaire page before 31 December 2021:

https://ec.europa.eu/eusurvey/runner/ECMWFNewslettersurvey2021.

Many thanks!

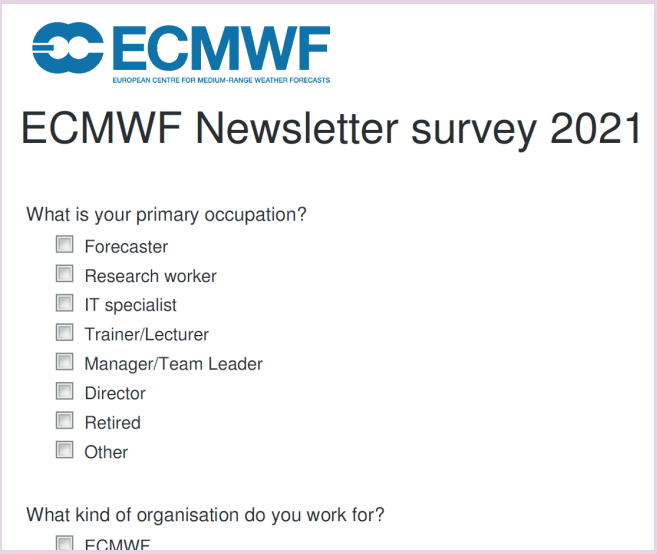

ECMWF supports Croatian met service during data centre move

Kristian Horvath, Endi Keresturi, Antonio Stanešić (all DHMZ), Xavier Abellan, Umberto Modigliani (both ECMWF)

After the earthquake that hit Croatia in 2020 and damaged its headquarters in Zagreb, the Croatian Meteorological and Hydrological Service (DHMZ) started a process to relocate its offices and data centre to new premises. This project reached an important milestone in July 2021, when all the remaining IT infrastructure was successfully moved to its new home. During the relocation of DHMZ's high-performance computing facility (HPCF) and archive, ECMWF's own HPCF and the European Weather Cloud were used to bridge the gap. This arrangement ensured DHMZ could carry on with its official duties, providing forecast services without any noticeable disruption to its end users. The solution built on the experience gained after the disaster occurred, when an emergency backup had to be implemented in a matter of days (see ECMWF Newsletter No. 164). This time, however, the schedule for the move was well known, so everything could be appropriately organised, prepared, and tested weeks in advance.

ECMWF's HPCF and the European Weather Cloud

To ensure that all users continued to receive prognostic products, the backup prognostic system at ECMWF's HPCF was reactivated. It consists of two ALADIN model configurations: one with a horizontal grid spacing of 4 km across a larger domain, and the other with a horizontal grid spacing of 2 km across a smaller domain, covering the broad area of Croatia. The initial conditions for both configurations are obtained from an unperturbed member of A-LAEF (ALARO - Limited Area Ensemble Forecasting), based on ALADIN's canonical model configuration ALARO, while coupling files come from the high-resolution system (HRES) of ECMWF's Integrated Forecasting System (IFS), taking advantage of data locality as both are produced on ECMWF's

DHMZ's supercomputer. A section of the SGI UV 2000 supercomputer system used by DHMZ.

HPCF. On this occasion, the list of products generated by these suites could be extended to satisfy the requirements of almost all DHMZ end users.

For the first time at DHMZ, all post-processing routines were implemented using ecFlow running on ECGATE. It was seen as a great opportunity to design, implement and test an ecFlow suite in a production context. The experience has been very positive, and DHMZ plans to extend the use of ecFlow to all operations in the future. Additionally, the suite was promoted to enjoy time-critical priority on ECMWF's HPCF during the preparation and the active backup period. This ensured minimal waiting times and timely production and delivery of products to the end users.

Several weeks before the relocation of computing infrastructure, a first notice was sent to customers. After that, new products were tested by some of the more advanced customers. Since some products for internal DHMZ users were stored on servers that were about to be moved, it was agreed that they would move to new locations. One location was a server located in the new DHMZ headquarters, and the other was a virtual machine on the European Weather Cloud. For external customers, the switch to the backup solution could be made completely transparent. DHMZ received a lot of appreciation from end users, who did not even feel this change in their weather-related applications, and showed that even in such challenging moments it can provide uninterrupted support.

Successful migration

The magnitude 5.5 earthquake on 22 March 2020, which was followed by eight strong aftershocks above magnitude 3.0 in the following days, caused considerable damage to the early 19th-century building hosting DHMZ in Zagreb at the time. The building was deemed unsafe to work in, but staff managed to carry on with their duties remotely and deliver the service to the public, relevant authorities, and critical end users. Several months after the earthquake, the relocation of employees to a new location was organised. However, most of the IT equipment continued to operate in the old building until it could finally be safely moved to the new premises. The new premises for the supercomputer system and archive system (tapes and disks) are in a modern data centre, while other servers were moved to the new DHMZ headquarters.

Thanks to close liaison and careful planning between DHMZ and ECMWF teams throughout this delicate process, the migration completed successfully without any service interruption. From DHMZ's side, in addition to the authors of this article, several other colleagues should be acknowledged for their hard work before, during and after the relocation: S. Panežić, A. Šljivić, M. Hrastinski, I. Odak Plenković and I. Muić.

ECMWF Support Portal – for all users and queries

Hélène Blanchonnet

ECMWF recently launched the ECMWF Support Portal as the primary entry point for all users for all types of queries on ECMWF data, products, and services (https://support.ecmwf.int). The aim is to give easy access to relevant pieces of documentation, allowing users to quickly find relevant answers to their queries. Should the query not be resolved, the Portal also offers the option to create support tickets, when appropriate. Soon, it will no longer be possible to send an email to the ECMWF Service Desk, and all support requests will be created via the ECMWF Support Portal.

How it works

The Support Portal is a web interface with a landing page that searches documentation and presents relevant articles and information offering solutions on common user issues, ranging from “how to reset your password” and “what is a reanalysis?” to “how to write a MARS request using web API”.

The landing page of the portal also allows users to select the topic of their issue by category:

- ‘Login and authentication’ – issues with logins to ECMWF systems and services
- ‘Charts and data’ – issues or questions relating to ECMWF charts and data, for example: downloading MARS data, using the Copernicus Climate Data Store, buying a licence for data, real-time dissemination issues, etc.
- ‘Software and computing’ – reporting any issues with a piece of software or the high-performance computing facility (HPCF) or getting access to ECMWF infrastructure services
- ‘Other issues’ – for anything else.

By selecting a category, commonly accessed articles are highlighted, and a more focused search can be done in the user documentation within the area of interest.

If users are unable to find the solution to their issue in user documentation, they can log in to the ECMWF system and create a support ticket (ECMWF registration is free of charge and open to all our users). This interface then either assigns the ticket to ECMWF Service Desk, who triage and assign it to the appropriate team, or in some cases the Support Portal can assign it to the relevant team directly.

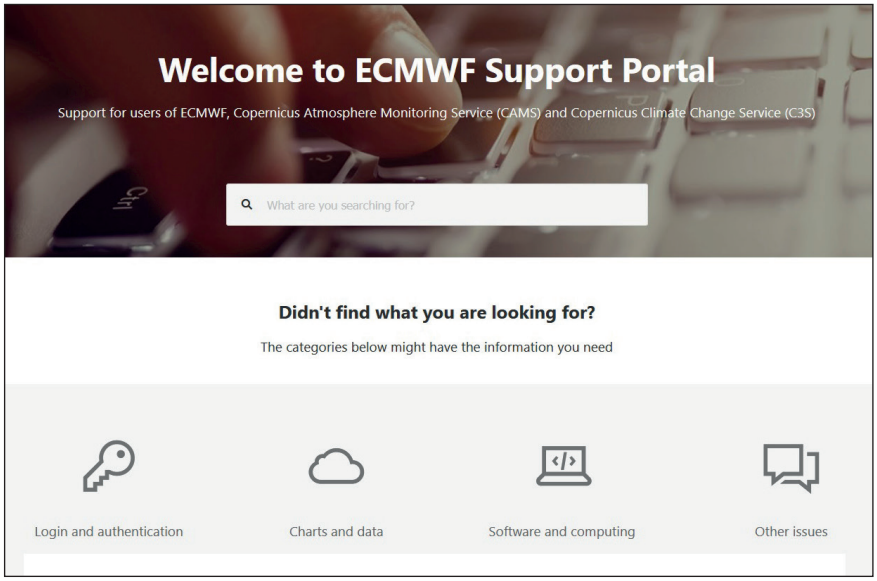

ECMWF Support Portal page. The landing page of the ECMWF Support Portal, where users can search for their query using the search box or by selecting the relevant category.

For example, if a user has a question about Copernicus Atmosphere Monitoring Service (CAMS) or Copernicus Climate Change Service (C3S) data, they would choose the ‘Charts and data’ category. On the next page, by typing their question in the search box, they would be presented with links to relevant articles. If the articles presented do not provide the appropriate answer, the user can create a support ticket by clicking on ‘Get our products’. When ‘Get our products’ is chosen, the support ticket is assigned directly to the Data Support team by the Support Portal. Whatever option is chosen by the users, the ticket can be manually assigned to the correct team if necessary.

As the use of the Support Portal increases, options will be refined to fit user needs and improve usability and efficacy. Several improvements are already planned before the end of the year, for example adding options during ticket creation to help the triage process and making it easier for users to give feedback on the Support Portal.

Serving all users

ECMWF has many users, including Member and Co-operating States, researchers and commercial users. They all have their own specific needs for support when it comes to using ECMWF data, charts, software and the HPCF, and they make use of many of the products and services ECMWF provides. Until recently each area of support had its own specific entry point for requesting support. This was confusing for users as they needed to know who to contact and how to go about it to get support.

The ECMWF Support Portal has introduced an initial entry point for all support request types. It aims to make support more effective and to reduce the need of manual intervention for common issues. This, we believe, will allow us to serve more users, providing high-quality support.

The Climate Data Store Virtual Assistant

Kevin Marsh, Michela Giusti, Xiaobo Yang, Anabelle Guillory

The Climate Data Store (CDS) is the cornerstone of the Copernicus Climate Change Service (C3S) at ECMWF. It serves tens of thousands of users, providing a wide range of free and open datasets and toolbox applications, which offer easy access to a wealth of climate information. The CDS Virtual Assistant (VA), or 'Knowledge Duck', is an exciting new addition to the support provided to C3S users. It can now be seen in action on CDS web pages: https://cds.climate.copernicus.eu/.

Role of the Knowledge Duck

User support is an important part of C3S. Various support channels have been set up in recent years as C3S has developed. These include the Knowledge Base, the User Forum, and the Jira-based service desk. Although users can access any one of these channels at any time, it can sometimes be confusing for them to know which one is best to find the answers they need. Therefore, to be better supported in their journey, our users need some guidance to explore the various information sources available. The VA will help ensure maximum and efficient usage of these support resources.

Prior to the introduction of the VA, the concept was tested by the development of a Support Beacon on the C3S website, which allowed users to access relevant pages from the Knowledge Base, and to raise Jira tickets without leaving the C3S website. This new VA is a significant improvement on the Support Beacon, which only provided simple searches of Knowledge Base content. By clicking on the Knowledge Duck icon in the corner of CDS web pages, a pop-up window will open and users can interact directly with the VA (see the screenshot). It provides answers drawn from the Knowledge Base and the User Forum, as well as the ECMWF parameter database and existing documentation stored on the CDS itself. Several pre-configured buttons also allow users to access answers to frequently asked questions about popular areas of interest, such as user accounts, ERA5, CDS API etc. The VA thus enables users to get considerable support whenever they use the CDS.

The VA is currently able to handle hundreds of simultaneous users, but it could be set up to deal with more. It was launched on the CDS on 1 July 2021, and the text box shows key statistics for the first two months of use. It should be noted that these are preliminary statistics. As the VA is an evolving system, a more representative picture will emerge after the system has been in use for a longer period. A full assessment will be produced in 12 months to verify the success of the system.

The Data Support Team monitors user interactions on a daily basis and improves the responses of the VA by either modifying existing responses or adding new ones. Users are invited to provide direct feedback about their interaction with the VA by rating the response they receive. Almost 50% of the feedback received in the first two months was positive, and 15% indicated that the interaction was somewhat useful. Around 25% of the feedback was negative, and no opinion was provided for the remainder. This feedback is also analysed every day by the Data Support team, and the responses from the VA are adjusted so that conversations which led to negative feedback are addressed as quickly as possible. This leads to a rapid improvement in the quality and usefulness of responses from the VA.

Over the first two months of the service, it has been seen that the questions asked by users have increased in complexity, with more conditional free-text questions being asked. While such free-text questions can be challenging for any automated system to answer fully, by constantly improving the responses from the VA it is more likely that the correct information will reach the user. If a user fails to receive a suitable answer from the VA, they are reminded that they can always submit their query via the

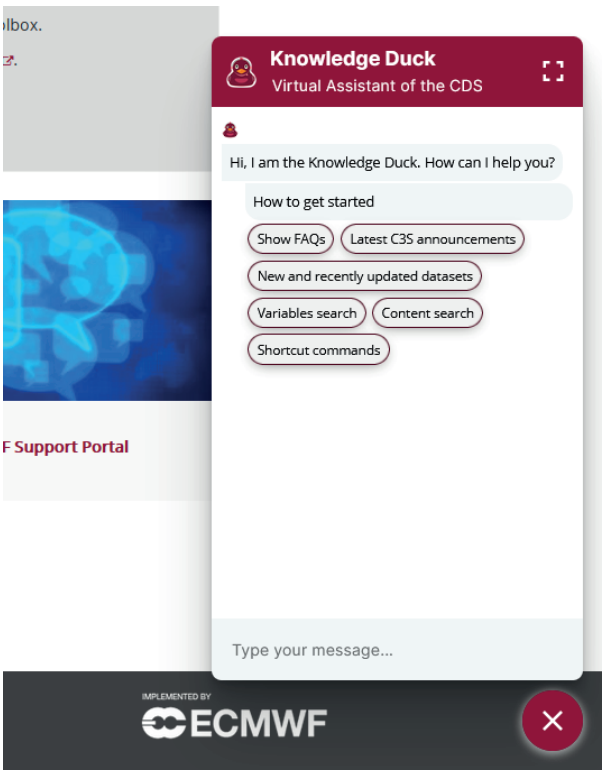

The Knowledge Duck. Located on the bottom right of CDS web pages, the Knowledge Duck can provide answers to common questions of CDS users.

ECMWF Support Portal (see the article on the Portal).

Outlook

In the future, the VA will continue to develop and evolve in several ways. The range of information sources used will be extended in order to provide answers to more complex user questions. In some cases, it would also be useful to have a 'person' behind the service, so that they could either interact with the user directly, or 'inject' a customised response into a user conversation. The system for detecting complex questions or negative feedback could also be improved so that a more agile service can be provided. There is also the possibility of allowing users to raise a Jira query directly from a VA conversation. It is hoped that eventually VAs may be used on the website of the Copernicus Atmosphere Monitoring Serivce (CAMS) and other ECMWF systems to complement existing user support services. Moreover, this may then allow user interactions to be transferred between them (or to retrieve answers from relevant VAs) to provide users with the information they need.

The CDS VA may be a small duck, but it has a very promising future, helping users to navigate the exciting waters of user support!

July–August 2021 stats

138,000 views 7,300 interactions	49.4% of feedback provided was positive
Top 3 countries: China, UK, Italy	**Top questions:** Dataset update information, variable definitions, CDS system status

CDS Virtual Assistant statistics. The chart summarises VA statistics from July to August 2021.

2022 Training Courses: registrations close soon

Sarah Keeley, Becky Hemingway

For the coming spring training season at ECMWF, we have expanded our training opportunities. All training for the new year is planned to be at the ECMWF headquarters in Reading. However, as the last two COVID-19 years have shown, we will have to adapt plans to the global situation nearer the time. We will also continue the two-level access pilot scheme for our Parametrization and Predictability courses so that it is possible to register as just a virtual attendee. The new 'Hands-on introduction to numerical weather prediction models' will be expanded to a five-day course this year after the positive feedback we received from participants.

There will be two new elements in 2022. As the new supercomputer system comes online in Bologna, there will be high-performance computer training for the Atos machine, which will run in March. In addition, a four-day machine learning course is being run for the first time in May. It will focus on machine learning for weather prediction.

The deadline for applications is fast approaching (29 October), so please apply soon. You can do so by accessing the 'Registration' page for the relevant course, a full online list of which can be found here: https://events.ecmwf.int/category/1/. We aim to process the applications with Member State endorsements by December so that people have enough time to make travel arrangements. We hope to be able to welcome you in person to a training event in 2022!

07 Feb – 10 Feb	Use and interpretation of ECMWF products
28 Feb – 04 Mar	Data assimilation
07 Mar – 11 Mar	EUMETSAT/ECMWF NWP-SAF satellite data assimilation
14 Mar – 18 Mar	High-performance computing – Atos
21 Mar – 25 Mar	Predictability and ensemble forecast systems
28 Mar – 01 Apr	Parametrization of subgrid physical processes
25 Apr – 29 Apr	Advanced numerical methods for Earth system modelling
03 May – 06 May	Machine learning for weather prediction
16 May – 20 May	A hands-on introduction to numerical weather prediction models: understanding and experimenting
03 Oct – 06 Oct	Use and interpretation of ECMWF products

Working on tropical cyclone predictions at ECMWF

Sharan Majumdar (University of Miami, US)

Sharan Majumdar. His research in tropical cyclones aligns with ECMWF's interest in evaluating its forecasts of these destructive storms.

After spending nearly 20 years as a professor at the University of Miami, and having focused on administration and teaching instead of writing research code during the 2010s, it was time to redress the balance by taking a sabbatical year. Since my early career was built on collaboratively using ECMWF ensemble data (for aircraft mission planning, targeted observations, probabilistic prediction, verification, predictability), my choice of institution was ECMWF.
My research is in tropical cyclones, which aligns with ECMWF's interest in evaluating its forecasts of these destructive storms. Several other agencies worldwide have invested in improving tropical cyclone prediction, and their track forecasts have caught up with ECMWF. These agencies have also prioritised genesis and intensity prediction, two areas of interest for me. For my future research and for use at ECMWF, I proposed to develop a 'toolbox' to diagnose these predictions. A sabbatical plan between June 2020 and July 2021 was accordingly developed and approved.

Diagnosing tropical cyclones

As COVID-19 turned the world upside-down in 2020, I adopted a sofa in a flat in central Reading as my new office. I used the adversity to quietly write volumes of Python code. This was first used to diagnose ECMWF's tropical cyclone forecasts and their errors in real-time, and to provide graphics to support a field campaign during the active Atlantic hurricane season. Everyone whom I met online was welcoming, especially the Diagnostics team during its thrice-weekly meetings. Not much more could have been done to foster collaborative discussions. However, being entirely online did reduce my learning efficiency, and it was challenging to immerse deeply within ECMWF, including the more subtle and organic aspects of its successful culture. I did observe with admiration how ECMWF pivoted into the new virtual world, including frequent communications across staff and management. Coupled with supervising students and new strategic planning duties at my university, the long days on my laptop were tiring but productive.

In 2021, a new Special Topic paper on tropical cyclones for the Scientific Advisory Committee (SAC) provided a target. I enjoyed diagnosing a suite of coordinated modelling and assimilation experiments for an active period during 2020, and it provided the opportunity to meet with additional experts at ECMWF. Led by Linus Magnusson, a paper has just been completed. This study provided several scientific outcomes. For genesis, the results were mixed. When a precursor disturbance is robust and isolated, the predictability and probabilistic skill of genesis is relatively high. However, genesis often occurs from initially small-scale, convectively disorganized waves, or waves that are interacting. Ensemble forecasts usually underpredict the probability of these genesis events. For tropical cyclone motion, in addition to a known slow

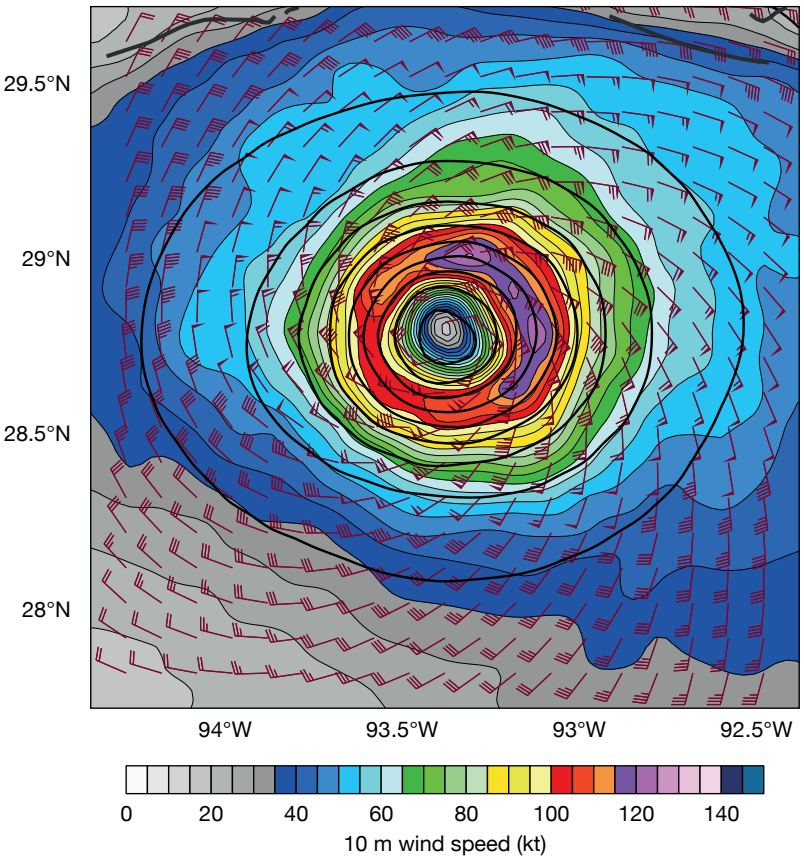

Simulating Hurricane Laura. The plot shows a 4 km experimental simulation of Hurricane Laura (2020), initialised from the operational analysis at 12 UTC on 24 August 2020, valid at 00 UTC on 27 August 2020.

bias, the largest errors usually arise in cases when the tropical cyclone is gaining latitude. Forecasts of both the position and intensity are also dependent on the initial motion, structure, and intensity of the tropical cyclone. Part of my toolbox depicts the three-dimensional anatomy of a tropical cyclone, in a cylindrical polar coordinate framework. It was especially pleasing to see realistic eyewall and rainband structures of intense hurricanes when the grid spacing was reduced to 4 km. Investigations of the structures also yielded insights on how the assimilation of selected observational datasets influenced analyses and forecasts. Since genesis and intensity change can be dominated by processes in the order of 1–10 km, limitations in the resolution of the data assimilation led to compromised representations of the physical processes. At the end of our paper, we make several recommendations. We are also planning to submit manuscripts for peer review.

What next?

Tropical cyclone forecasting will continue to provide challenges on all timescales, and will serve as 'stress tests' for versions of ECMWF's Integrated Forecasting System (IFS) under development. I look forward to continued collaborations with ECMWF to diagnose their forecast errors and uncertainties, to help keep advancing predictive skill. Another interest is to expand to wind and rainfall structure, and their impacts. Finally, I would like to thank my primary collaborator and friend Linus Magnusson, David Richardson and ECMWF management for supporting the visit, the University of Miami for granting the sabbatical leave, and the US National Science Foundation and Office of Naval Research.

ECMWF becomes a multi-site organisation

ECMWF has officially become a multi-site organisation after the opening ceremonies for offices in Bonn, Germany, on 13 September and its data centre in Bologna, Italy, on 14 September 2021. This marks an exciting new phase for ECMWF, strengthening ties with its Member States through new locations in Europe in addition to its existing UK headquarters, and the first step towards upgrading its already world-class supercomputing capability to advance its forecasts.

Bonn

Following an international tender amongst its Member States, ECMWF opened a site in Bonn, a city already known as home to several international and intergovernmental organisations. The focus in Bonn is work conducted in partnership with the European Union (EU), including the Copernicus Earth observation programme and the planned Destination Earth initiative. The location in Bonn also enables further collaboration with scientific institutions across Germany and the region, and closer connection with ECMWF Member States. In particular, ECMWF will collaborate with the Center for Earth System Observations and Computational analysis (CESOC), which integrates research at the Universities of Bonn and Cologne as well as the Forschungszentrum Jülich. From 2022, a visiting scientist programme, targeting activities in Bonn, will also begin. The ECMWF flag will fly outside the Ministry for the Environment, Nature Conservation and Nuclear Safety (BMU) headquarters, the organisation's new home before it transfers to a brand-new building in 2026.

Bologna

ECMWF's data centre in Bologna houses the Centre's new Atos BullSequana supercomputer system, scheduled to begin running operationally in 2022. The new system will increase sustained performance by a factor of about five compared to ECMWF's current high-performance computing facility. It provides the flexibility to accommodate the latest technologies in supercomputing. It will also facilitate the continuation of investigative work into the field of machine learning in numerical weather prediction, as well as the use of advanced high-performance computing, big data and AI methodologies to create a digital twin of the Earth with a breakthrough in realism. The data centre is on the site of the Tecnopolo di Bologna campus, which is redeveloping the unused buildings and grounds of a former tobacco factory.

ECMWF Summer of Weather Code drives open-source developments and innovation

Julia Wagemann, Esperanza Cuartero

The fourth edition of ECMWF's Summer of Weather Code (ESoWC) came to a close with the Final ESoWC Day on 29 September 2021. The day-long online event showcased the outcomes of nine open-source projects, which nine developer teams worked on during a four-month coding period from May to August 2021. This year's projects were at the intersection of machine learning, web development, visualisation, data compression and open data exploration.

Overview

Four projects concerned advancing machine learning in Earth system science:

- **MaLePoM: Machine Learning for Pollution Monitoring**

  Nicolo Brunello, Vidur Mithal, Paolo Fornoni and Luca Rampini implemented a machine learning workflow to estimate NOx emissions with the help of suitable proxy data from anthropogenic activities, such as dynamic traffic data and others.

- **ML4Land: Using Earth observation data, climate reanalysis and machine learning to detect Earth's heating patterns**

  Avishree Khare and Het Shah developed a machine learning model that predicts land surface temperature based on ERA5 climate reanalysis variables on a regional scale.

- **AQ Bias Correction**

  Antonio Perez Velsco and Mario Santa Cruz Lopez explored the use of machine learning in order to adjust biases between models and observations in air quality forecasts.

- **CliMetLab: Machine learning on weather and climate data**

  CliMetLab is an early-stage open-source Python package that aims to simplify meteorological and climate data preparation for machine learning projects. Ashwin Samudre helped to implement some important features that will help to enhance the functionalities of the package.

Three projects had a focus on web development and improving the visualisation of weather data:

- **ECMWF User Dashboard**

  Varun Bankar developed an interactive user dashboard, which allows ECMWF users to choose and load different services, e.g. ECMWF web charts, and customize their dashboard view.

- **BlenderNC enhancements**

  Tisham Dhar, Gichini Ngaruiya and Josue Martinez Moreno enhanced the BlenderNC software to support the loading of GRIB files. This is an important step forward to increase the use of BlenderNC in the meteorological community to make long-lasting visualisations with weather data.

- **Meeresvogel**

  Kathryn Schmitt developed additional functionalities for Google Earth to be able to better represent meteorological information, such as wind or mean sea level pressure. These light-weight features will be very useful for sailors, who need fast and easy access to such information.

Another two projects, concerning data compression and open data exploration, focused on atmospheric composition data:

- **Elefridge.jl: Compressing atmospheric data into its real information content**

  This project was already part of ESoWC 2020, and Milan Kloewer continued his work on exploring the potential of compressing atmospheric data while preserving real information to reduce storage and to facilitate data sharing. It provided evidence that the size of climate and weather forecast data archives can be reduced by one to two orders of magnitude without losing valuable information.

- **ADC Toolbox: Comparing Atmospheric Composition Datasets**

  Alba Vilanova Cortezon developed a Python-based toolbox which facilitates the comparison of satellite- and model-based data on atmospheric composition, such as data from the Copernicus Atmosphere Monitoring Service (CAMS) and from the GOME-2 and IASI instruments onboard the polar-orbiting Metop-ABC satellites.

High-quality outcomes

At the core of the ECMWF Summer of Weather Code is the provision of

innovative and open-source software solutions as well as attracting external expertise and new talents. ESoWC is known for the high standard of open-source solutions being developed during the coding phase. These high-quality outcomes are supported by a strong mentorship offered to the participating teams by ECMWF and Copernicus mentors. The collaborations often continue after the official end of an ESoWC edition.

ECMWF Summer of Weather Code was initiated in 2018. Since then, the programme has constantly grown through strategic partnerships with the two Copernicus services at ECMWF as well as two European cloud services: the European Weather Cloud and the Copernicus DIAS service WEkEO. These partnerships support ESoWC in its mission to drive innovation and open-source software developments in the meteorological and climate community.

ECMWF Summer of Weather Code will continue in 2022, and further information will be announced on the programme's website (https://esowc.ecmwf.int/), on Github (https://github.com/esowc) and on Twitter (https://twitter.com/esowc_ECMWF).

ECMWF helps EUCOS to monitor observations

Ersagun Kuşcu, Cristina Prates, Thomas Haiden

In-situ observations are an important ingredient of numerical weather prediction (NWP). Their availability, timeliness, and quality determine their usefulness in data assimilation and thereby affect the skill of numerical weather forecasts. In Europe, EUMETNET, a network of national meteorological services, operates and develops the EUMETNET Composite Observing System (EUCOS), which in turn makes a major regional contribution to the World Meteorological Organization (WMO) Integrated Global Observing System (WIGOS). ECMWF helps EUCOS to achieve its aims by providing quality monitoring results of in-situ observations that are available in the Integrated Forecasting System (IFS).

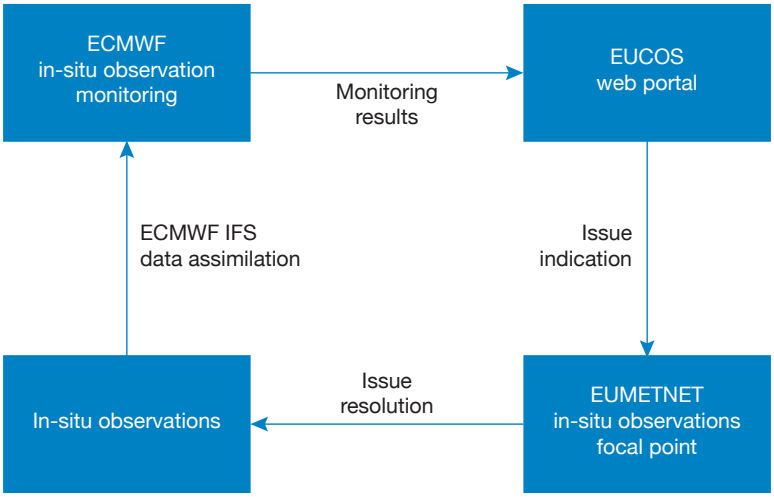

EUCOS feedback loop between observation monitoring and NWP. Issues detected by monitoring observations are published, triggering action towards resolution, which also benefits NWP.

Originally created as an operational network in 2002, EUCOS established collaboration across much of Europe with the aim of optimising surface-based observation activities to improve the quality and cost-effectiveness of NWP at the European scale. Achieving this goal requires day-to-day monitoring of observation availability and quality as well as rapid feedback to data providers in case of missing or erroneous observations. ECMWF's role is to provide comprehensive observation monitoring statistics to EUCOS on a daily basis, such that action can be taken close to real time if an issue is identified. ECMWF is in a good position to do so because of its advanced data assimilation and observation quality control systems.

Observation types for which ECMWF provides monitoring information to EUCOS are SYNOP (weather observations from ground stations), SHIP (ship-based surface meteorological observations), PROFILER (vertical profiles of wind), BUOY (surface meteorological observations provided by moored and drifting buoys), TEMP (radiosonde reports)/ASAP (Automated Shipboard Aerological Programme), and AMDAR (Aircraft Meteorological Data Relay). Metrics typically include background departures, analysis departures, and usage status. In the case of TEMPs, for example, these are provided for the parameters of temperature, relative humidity, and vector wind. While a single large departure may be due to either an observational or model problem, a step-change increase in departures over several assimilation cycles often indicates an observational issue. In this way observation providers benefit from NWP, which in turn benefits from using their observations. This feedback loop is illustrated by the figure.

Because of its successful operation, EUCOS observation monitoring has served as a model for the WIGOS Data Quality Management System (WDQMS), which aims to expand the EUCOS concept to the whole globe, again with strong involvement of ECMWF in the monitoring component. In this case the monitoring information is received by the WIGOS Regional Centres, which then contact data providers so they can initiate corrective action. WDQMS is still in the process of being fully established, and it is expected that its operation will lead to another major improvement in the quality and reliability of meteorological in-situ observations worldwide.

ECMWF contributes to new Earth system models

Irina Sandu (ECMWF), Bjorn Stevens (Max-Planck-Institut für Meteorologie, Germany)

ECMWF is taking part in NextGEMS, a project that started on 1 September and is funded by the European Commission's Horizon 2020 programme. Over the next four years, NextGEMS will develop a new generation of Earth system models and use them to help fill gaps in our understanding of how the Earth system works and how the world's climate will change over the next three decades. NextGEMS will also form the nucleus of a next-generation, more cooperative and pan-European approach to Earth system modelling, by involving 26 partners in 15 countries.

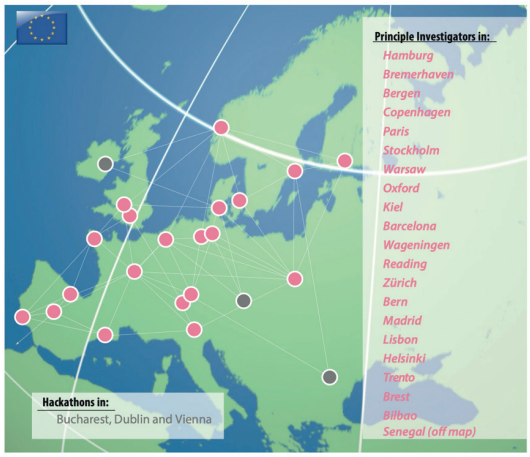

NextGEMS participants. The map shows NextGEMS partners (magenta circles) and hackathons planned for non-partner institutions (grey circles). The lead coordinator will be Bjorn Stevens (Max-Planck-Institut für Meteorologie, MPI-M), Irina Sandu (ECMWF) will act as co-coordinator, and the NextGEMS project office will be at MPI-M.

Main goals

NextGEMS aims to substantially increase the realism of Earth system simulations by developing two global storm-resolving Earth system models with resolutions of 2 to 5 km in the atmosphere and ocean. At these resolutions, important phenomena which are either neglected or need to be parametrized in today's weather and climate models become explicitly resolved. These include storms associated with precipitating deep convection, but also a range of other processes, such as ocean mesoscale eddies, the influence of mesoscale land-surface heterogeneity and of topography on large-scale atmospheric circulations, and water-mass formation in the ocean. These resolutions are also commensurate with scales familiar and more relevant to end users from impact sectors, such as risk assessment, renewable energy or marine fisheries.

Simulations at the scales envisaged in NextGEMS will underpin both operational ECMWF forecasts by the end of the decade, and European efforts to create replicas of the Earth system in the European Commission's Destination Earth programme. By developing these next-generation Earth system models, NextGEMS thus supports and contributes to ECMWF's and Europe's ambitions to significantly advance our prediction capabilities at all timescales.

To fully exploit the potential of NextGEMS storm-resolving models, a number of scientific challenges need to be overcome, related for example to the coupling between different Earth system components, the representation of processes which remain unresolved, or water and energy balance and conservation issues. ECMWF's participation in NextGEMS will allow us to focus on some of these challenges. We shall, for example, work on a more accurate representation of moist physics, and of the way the land and ocean are coupled to the atmosphere at the scales envisaged in NextGEMS. This will support the science agreed in the ECMWF Strategy 2021–2030.

New ways of working

The simulations envisaged in NextGEMS are only becoming possible thanks to recent advances in supercomputing technologies and to investments in the scalability of the models at the core of NextGEMS storm-resolving Earth system models: ICON, developed by the Max-Planck Institute for Meteorology and the German National Meteorological Service (DWD), and the Integrated Forecasting System (IFS) from ECMWF developed in partnership with Member States (coupled with the community ocean model NEMO and the Alfred Wegener Institute's FESOM2 ocean model). However, the huge computational and data demands of NextGEMS simulations require new and more inclusive ways of working. NextGEMS will develop new workflows to exploit these simulations and will use them to fill important knowledge gaps. To do so, it will make extensive use of knowledge co-production hackathons to advance model development, but also to develop pilot projects on near-surface renewable energy production and coastal marine ecosystems and fisheries. In these pilot projects, users from these sectors will closely interact with model developers to better tailor the simulation output to their needs and thus short-circuit the value chain.

New observations since July 2021

The following new observations have been activated in the operational ECMWF assimilation system since July 2021.

Observations	Main impact	Activation date
PMAP aerosol product from Metop-C	Aerosol in the CAMS system	19 July 2021
MISTRAL surface observations over Italy and Slovenia	Surface variables locally	6 August 2021

IFS upgrade improves moist physics and use of satellite observations

Richard Forbes, Patrick Laloyaux, Mark Rodwell

On 12 October, ECMWF implemented the second upgrade of its Integrated Forecasting System (IFS) in 2021. IFS Cycle 47r3 includes numerous changes to the forecast model, observation usage and data assimilation system, with contributions from many teams across the Centre. There are major developments to the representation of moist physics in the model and increased observation usage in cloudy regions in the assimilation. The upgrade improves the large-scale atmospheric circulation and reduces tropical cyclone track errors in both high-resolution (HRES) and ensemble (ENS) forecasts. Several forecast products are modified, such as visibility and wind gusts, and new products are introduced, including clear-air turbulence.

Data assimilation and observation usage

AMSU-A microwave temperature sounding observations in clear-sky conditions have been some of the most powerful observations assimilated into the IFS. Continuing our successful long-term strategy of an all-sky exploitation of satellite radiance observations, AMSU-A data are now assimilated in all-sky conditions (in clear, cloudy, and rainy situations). The increased data usage in cloudy regions leads to an improved fit to independent satellite and conventional observations, and an improvement in forecast scores. The filling of data gaps in cloudy regions is very clear in the case of tropical cyclone Humberto (Figure 1). Not only is coverage improved in the immediate vicinity of Humberto (indicated by the white circle) but also in the surrounding region, which is likely to be important for influencing its subsequent track (indicated by black crosses). Including AMSU-A in the all-sky assimilation is a major step towards an all-sky use of all passive microwave observations. With 47r3, the only passive microwave instrument assimilated in just clear-sky conditions will be ATMS, which is expected to be moved to all-sky assimilation shortly.

Radiative transfer 'RTTOV' calculations for hyperspectral infrared sounders now benefit from improved accuracy in the underlying line-by-line spectroscopy calculations, a finer vertical grid and more realistic CO_2 concentrations. Assimilation experiments

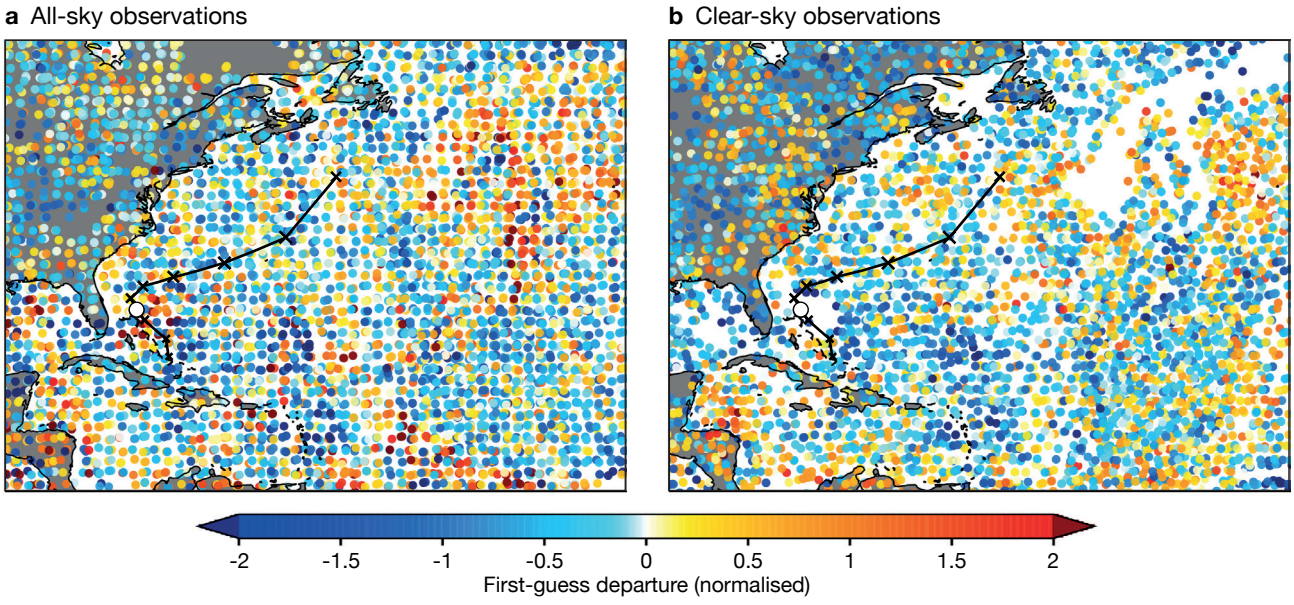

FIGURE 1 First-guess departures for (a) all-sky and (b) clear-sky channel 5 observations assimilated during the 12-hour long window starting at 00 UTC on 15 September 2019. The National Hurricane Center (NHC) best track locations at 00 UTC over the life of Humberto are given by a black X, with a white circle showing the hurricane location at 00 UTC on 15 September 2019, just east of Florida. Data from all AMSU-A platforms are shown together. Departures are normalised by the assigned observation errors.

doi: 10.21957/m3805gf17r

show that the new RTTOV (version 13.0) significantly improves the simulation of these observations and, as a result, the performance of the data assimilation system.

The assimilation of AIRS data now benefits from an updated observation error covariance matrix, including error correlations, bringing the use of AIRS in line with that of other hyperspectral infrared (IR) instruments.

Diagnostics highlighted a probable misassignment of the heights for some low-level Atmospheric Motion Vector (AMV) observations. In a new approach, low-level AMVs placed above model clouds are now reassigned to the level at the average pressure of the model cloud layer (Lean & Bormann, 2021). This has been found to give the best results compared to simply screening out affected AMVs or using the model cloud top or base when considering departure statistics and forecast skill. The change was also supported by independent wind profile observations from the Aeolus satellite. With this change, the AMV assimilation is expected to benefit from improvements in our cloud modelling, as well as from improvements in the height assignment provided by AMV producers.

Weak-constraint 4D-Var (WC-4DVar) has been implemented in the Ensemble of Data Assimilations (EDA) system, where the stratospheric temperature bias is corrected independently for each ensemble member. The reduction in the mean background and analysis errors is comparable to the impact obtained in the HRES analysis when WC-4DVar was introduced in Cycle 47r1, reducing the stratospheric temperature bias by up to 50%.

The European Space Agency's Doppler Wind Lidar Earth Explorer mission, Aeolus, is an important source of wind observations in clear and cloudy skies from the molecular (Rayleigh) and particle (Mie) channels. The impact of the Mie-cloudy winds is improved in Cycle 47r3 using an updated observation error assignment model, which accounts for representativeness error.

A package of mainly observation-related changes in the assimilation code includes the important introduction of NO_2 observations from the TROPOMI instrument on board the Copernicus Sentinel-5P satellite, using new NO_x code for the simplified chemistry in the tangent-linear and adjoint models.

Forecast model

The major revision to the physics in Cycle 47r3 (Figure 2) improves the physical and numerical basis for parametrized processes in the model associated with boundary layer turbulence, convection, subgrid saturation adjustment and cloud and precipitation microphysics. Their complicated interactions are described more simply, efficiently, consistently and scale-independently. The developments are a culmination of work spanning several years and are part of a long-term development of the moist physics in the IFS in preparation for the transition to higher horizontal resolutions (3–5 km) in future operations. The main changes are summarised here, and further details can be found in Bechtold et al. (2020).

- In the revised turbulence scheme, the methods of determining a clear or cloudy mixed layer and the heights of the mixed layer and cloud base are now consistent with those in the convection scheme. The calculation of the strength of the inversion at the top of the mixed layer has been revised, and the

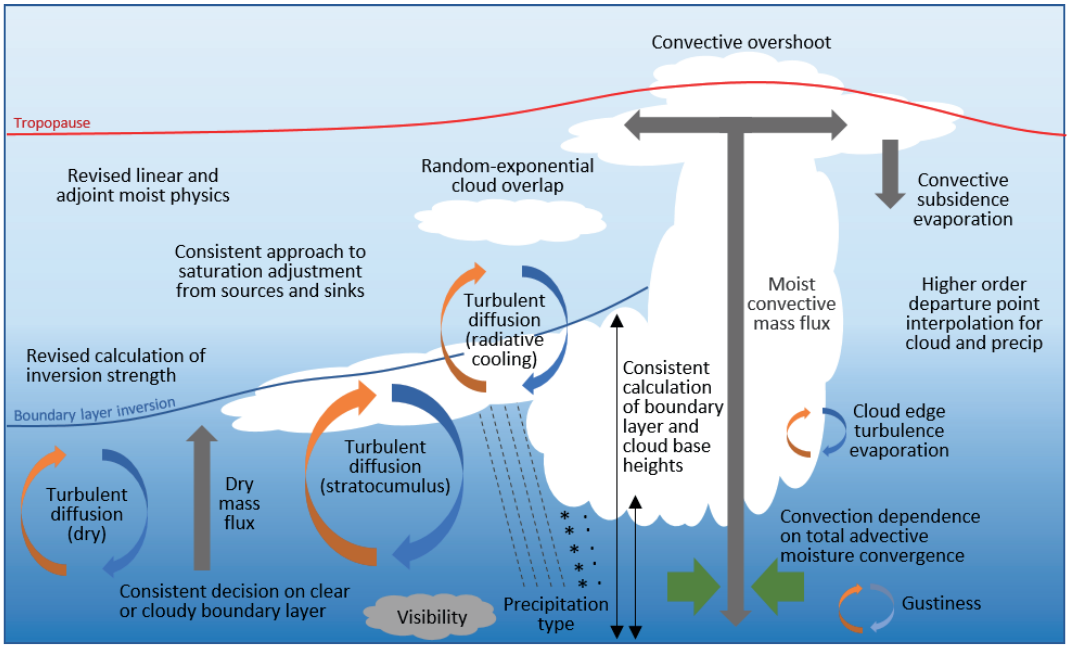

FIGURE 2 Schematic highlighting many of the turbulence, cloud and convection processes that have been modified in the moist physics upgrade in IFS Cycle 47r3.

47r3 HRES scorecard

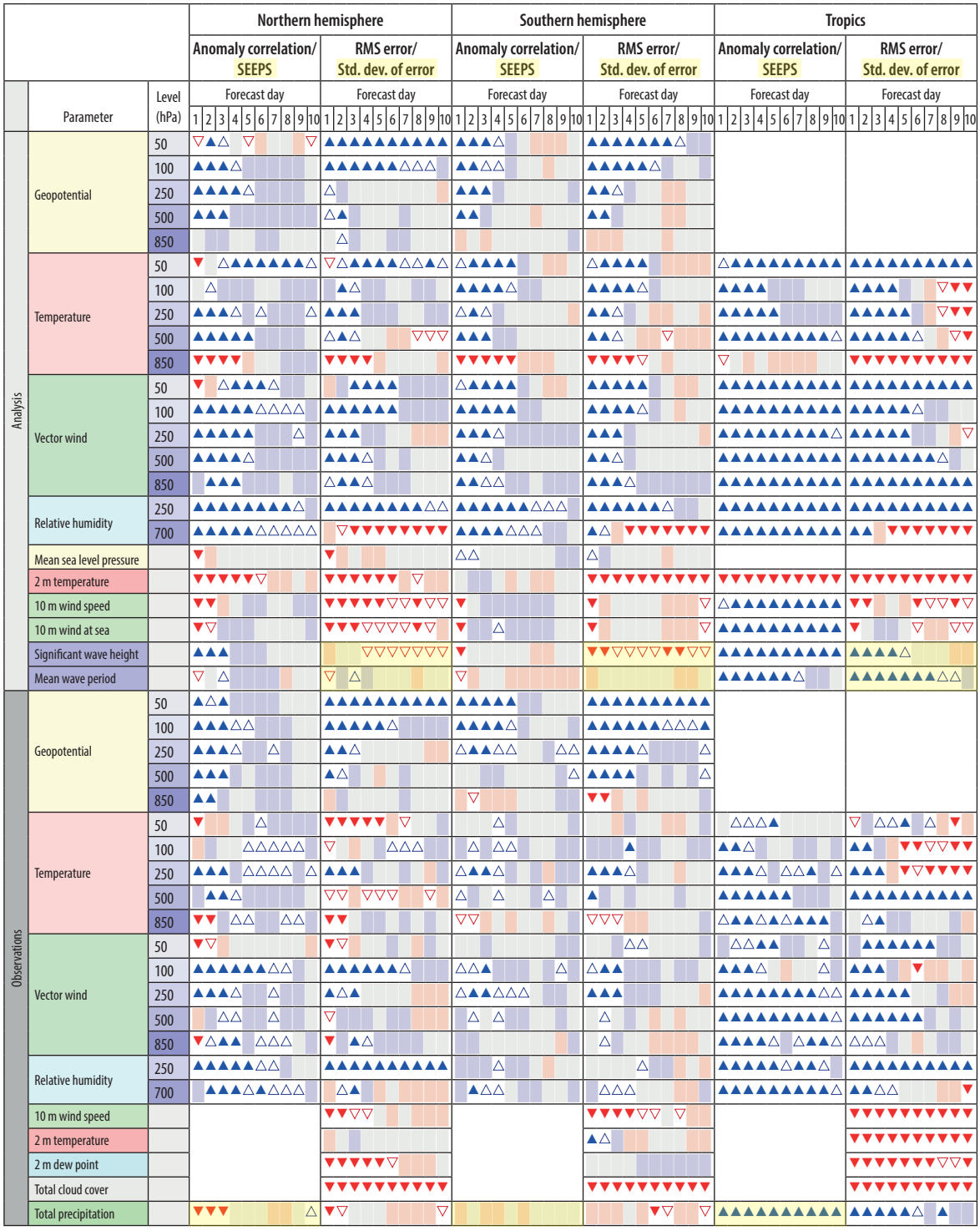

Symbol legend: for a given forecast step...

- ▲ 47r3 better than 47r2 statistically significant with 99.7% confidence
- △ 47r3 better than 47r2 statistically significant with 95% confidence
- 47r3 better than 47r2 statistically significant with 68% confidence
- no significant difference between 47r2 and 47r3
- 47r3 worse than 47r2 statistically significant with 68% confidence
- ▽ 47r3 worse than 47r2 statistically significant with 95% confidence
- ▼ 47r3 worse than 47r2 statistically significant with 99.7% confidence

FIGURE 3 HRES scorecard of IFS Cycle 47r3 versus IFS Cycle 47r2, verified by the respective analyses and observations at 00 and 12 UTC, based on about 650 forecast runs for the period June–August 2020 and December 2020–August 2021. The HRES is run at TCo1279 resolution, corresponding to a horizontal grid spacing of about 9 km, and with 137 levels.

saturation adjustment process from the turbulent mixing that was previously treated with a separate statistical cloud scheme is now treated more consistently with the prognostic cloud scheme.

- The formulation of the saturation adjustment (condensation/evaporation) process for partially cloudy grid boxes was revised and simplified with the removal of a first-guess adjustment before the convection scheme and more consistent assumptions for ice supersaturation in the clear-air part of the grid box. This affects cloud cover with a higher occurrence of fully cloudy grid boxes. The simplifications to the saturation adjustment facilitate future development of the moist physics processes and interactions.
- A stronger coupling of the convection parametrization with the dynamics, through total advective moisture convergence in the convective instability calculations, helps to improve the representation of mesoscale convective systems and their propagation, on average, at both current and future operational resolutions (Becker et al.). There are other impacts on the precipitation that are discussed in the next section.
- There are changes to the cloud vertical overlap parametrization used in the radiation scheme and total/high/medium/low cloud cover products. The overlap of two separated cloud layers was previously dependent on the exponential of separation distance but is now changed to random overlap, in agreement with observations. Overlap for model levels within a contiguous cloud are still treated with the exponential of separation approach. This generally acts to increase cloud cover, which is also modified by changes to the cloud edge turbulent erosion, subsidence evaporation and saturation adjustment.
- The semi-Lagrangian departure point interpolation is changed from linear to cubic for the advection of the cloud liquid, cloud ice, rain and snow prognostic variables to be consistent with the humidity and cloud fraction variables. A 3D quasi-monotone limiter is activated to avoid overshoots and negative values. The higher order interpolation leads to less numerical smoothing and smaller-scale structure of cloud and precipitation fields in the forecast.
- There are updates to the ensemble Stochastically Perturbed Parametrization Tendencies (SPPT) scheme to reduce the upper-tropospheric tropical temperature warm bias that arises from the addition of stochastic perturbations.
- The simplified moist physics formulation for the tangent-linear and adjoint model is an important part of the 4D variational assimilation system and has been updated in 47r3 to be more consistent with the revised physics parametrizations in the forecast model.

Impact on medium- and extended-range forecasts

The changes in Cycle 47r3 have been extensively tested across the different resolutions and configurations of the IFS at medium-range, extended-range and seasonal timescales. The extended-range ensemble was evaluated with forecasts initialised at the start of each month for the period 1989–2016. Case studies at the higher horizontal resolution of 4 km were also conducted to assess the impacts on future operational upgrades.

Figures 3 and 4 show medium-range scorecards for Cycle 47r3 relative to own analysis and observations, for the HRES and ENS, respectively (interactive scorecards are available from the 47r3 implementation web page: *https://confluence.ecmwf.int/display/FCST/Implementation+of+IFS+Cycle+47r3*). There are many positive impacts of the Cycle, particularly on upper-air scores and tropical cyclone tracks. There are also some deteriorations, and both are discussed below.

Upper-air geopotential and wind in the first few days of the forecast are significantly improved (Figure 5), by up to a few per cent for the northern hemisphere 500 hPa geopotential anomaly correlation, reducing with lead time. Upper-air winds are particularly improved in the tropics throughout the medium range, by up to 7%, reducing with lead time. Tropical upper-air temperatures are improved in HRES but degraded in the ENS from a small (~0.2 K) increase in bias due to a warming by the stochastic perturbations (partly mitigated by the SPPT changes mentioned above). Low level temperatures (including 850 hPa and 2 m temperature) are approximately neutral versus observations but degraded versus analyses in the subsidence regions over subtropical oceans, where the temperature at 850 hPa is very sensitive to small changes in boundary layer height.

For tropical cyclones, there is a 10% improvement in the track location errors in both HRES and in the ensemble mean of ENS (Figure 6) from forecast days 2 to 5, due to a combination of the additional observations assimilated in cloudy regions and model changes which improve the steering flow. With little change in spread, this results in an improvement in the statistical reliability of the tracks. The tropical cyclone central pressure is shallower on average by 2–3 hPa in Cycle 47r3. The difference can be greater than this in the rapidly deepening phase, with Cycle 47r2 closer to the ‘best-track’ central pressure data (reported by the official global monitoring centres), but of opposite sign in the later stages, where Cycle 47r3 is closer to the ‘best-track’ data. Tests at a higher resolution (4 km)

47r3 ENS scorecard

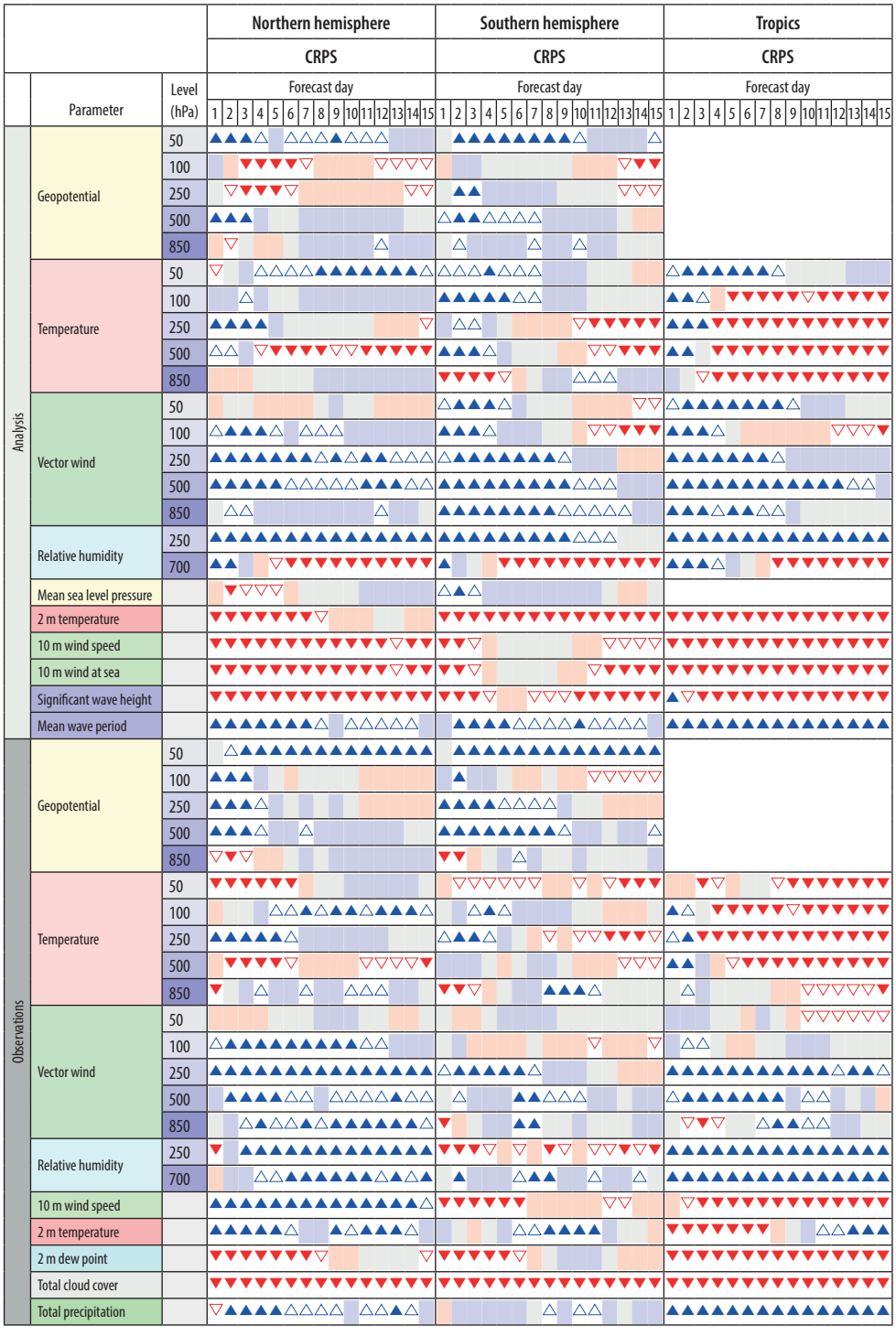

Symbol legend: for a given forecast step...

- ▲ 47r3 better than 47r2 statistically significant with 99.7% confidence
- △ 47r3 better than 47r2 statistically significant with 95% confidence
- 47r3 better than 47r2 statistically significant with 68% confidence
- no significant difference between 47r2 and 47r3
- 47r3 worse than 47r2 statistically significant with 68% confidence
- ▽ 47r3 worse than 47r2 statistically significant with 95% confidence
- ▼ 47r3 worse than 47r2 statistically significant with 99.7% confidence

FIGURE 4 ENS scorecard of IFS Cycle 47r3 versus IFS Cycle 47r2 for medium-range forecasts up to forecast day 15, verified by the respective analyses and observations at 00 UTC based on about 305 ENS forecast runs for the period June–August 2020 and December 2020–August 2021. The ENS is run at TCo639, corresponding to a horizontal grid spacing of about 18 km, and with 137 levels.

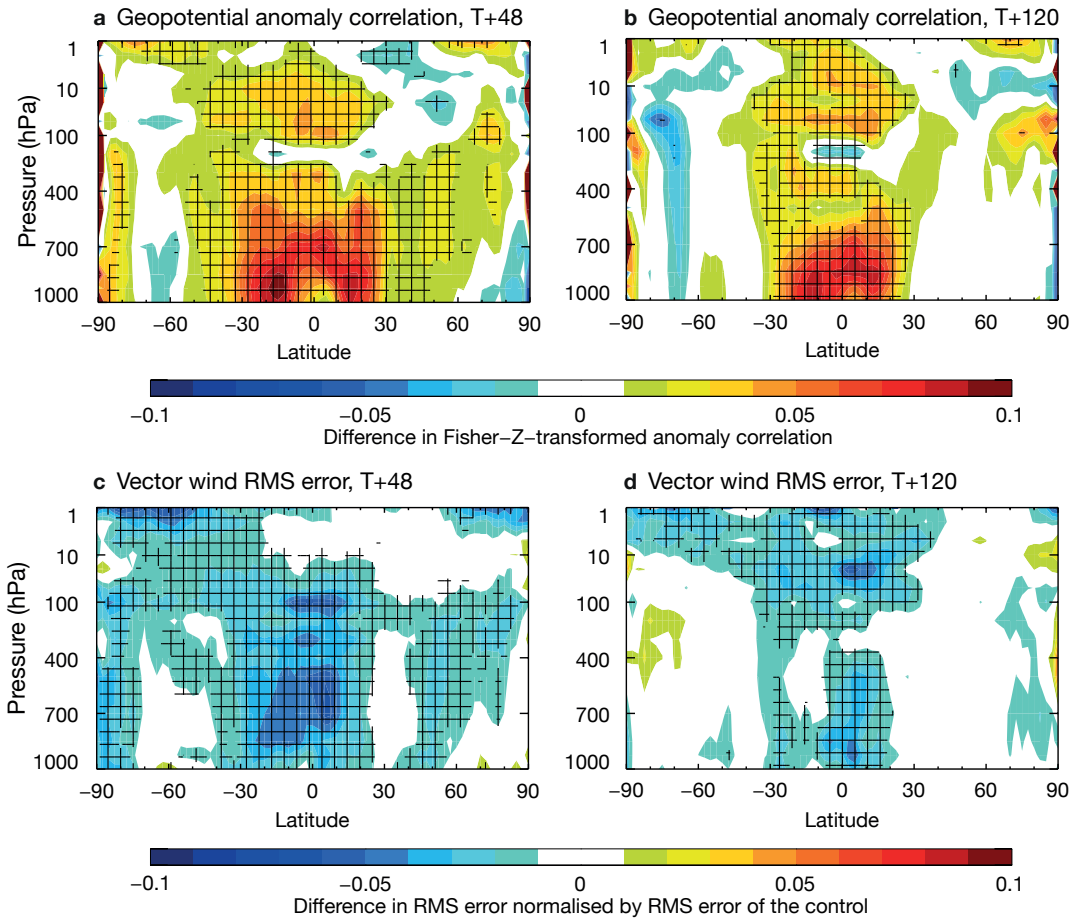

FIGURE 5 Zonal mean cross-sections of normalised difference in HRES between Cycle 47r3 and 47r2 of (a) geopotential anomaly correlation at forecast day 2, (b) the same at forecast day 5, (c) vector wind root-mean-square (RMS) error at forecast day 2 and (d) the same at forecast day 5. Positive values in (a) and (b) show improved anomaly correlation and negative values in (c) and (d) show reduced RMS error. Results are based on the period from June to August 2020 and December 2020 to April 2021. Hatched regions indicate statistical significance.

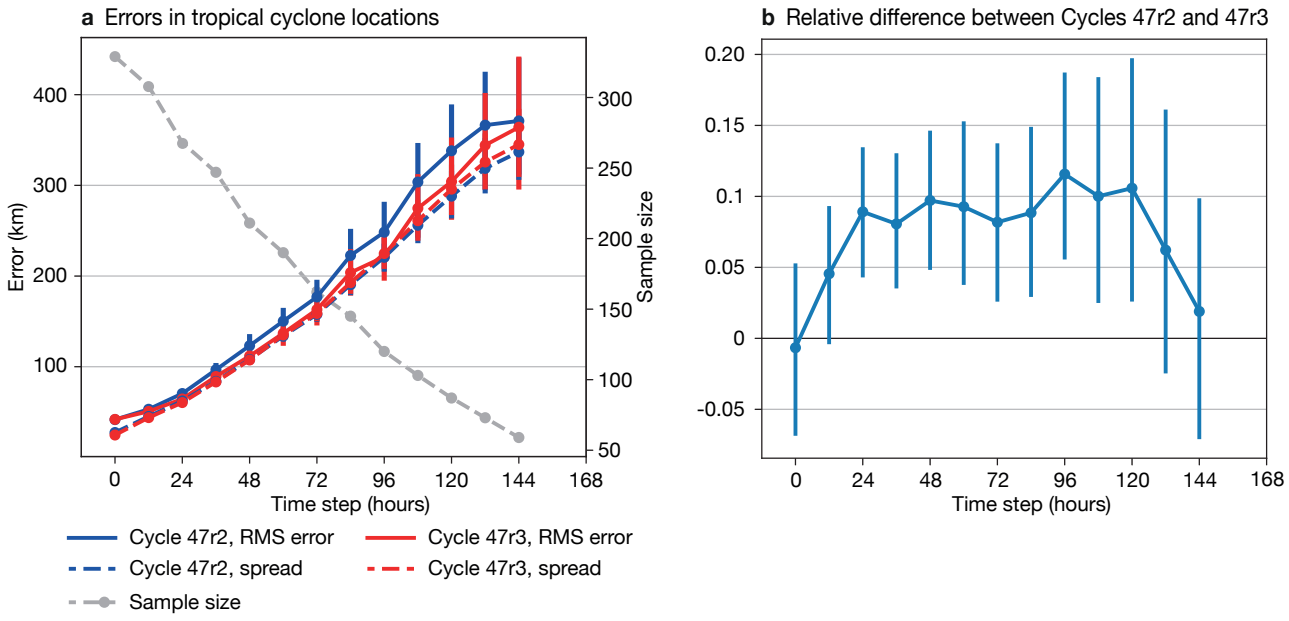

FIGURE 6 The charts show (a) root-mean-square (RMS) location errors (solid lines) in the ensemble mean of tropical cyclone positions in Cycle 47r2 (blue) and 47r3 (red), along with the standard deviation ('spread', dashed lines) among ensemble members, and (b) the normalised difference in ensemble mean location error between Cycles 47r2 and 47r3 (positive values indicate improved position in 47r3). Results are based on all TC basins for the period from 2 December 2020 to 30 August 2021. The dashed grey line in the left-hand panel and the right-hand side scale indicate the number of tropical cyclones which could be evaluated at each lead time. The bars indicate 95% confidence intervals.

show generally deeper tropical cyclones in both model versions, but Cycle 47r2 more frequently over-deepens, whereas Cycle 47r3 at 4 km resolution is in overall closer agreement with best-track central pressure values. The physics of Cycle 47r3 thus better prepares the IFS for future increases in horizontal resolution.

The impact on near-surface parameters is more mixed. There is a small improvement in 2 m temperature in the extratropics, but a small degradation in the tropics. Two-metre dew point and 10 m wind also show small deteriorations. A 3% increase in bias of total cloud cover as well as an increase in small scale variability and more binary (0/1) cloud cover leads to a degradation in the calculated scores. With such a major physics change, it is inevitable that there are some degradations, and these will be investigated further for later IFS cycles.

A key focus for the moist physics upgrade is precipitation. There are significant changes in the characteristics of precipitation, including enhanced fine-scale structures, reduced areal coverage and higher peak precipitation rates. The PDF (probability density function) of precipitation rate is improved, with reduced occurrence of light precipitation rates and increased occurrence of high precipitation rates in convective regimes, but similar precipitation accumulations overall. This is particularly evident over continental regions such as the USA and Africa, in better agreement with radar and satellite-based precipitation estimates. Along the intertropical convergence zone (ITCZ) there are reductions in the number of overactive quasi-stationary precipitation cells, which has been a longstanding problem in the IFS. The relative change in the 99th percentile for precipitation in the model climate at day 2 shows this reduction along the ITCZ (Figure 7). The figure also shows increased convective precipitation in semi-arid regions, for example reducing the dry bias around the Mediterranean in summer, but little change in the statistics of extreme precipitation accumulations in the rest of the extratropics.

The overall precipitation scores show some positive signals. For tropical precipitation, the HRES shows improvements of 1–2% in the deterministic SEEPS (stable equitable error in probability space) score, and the ENS shows improvements of about 0.6% in the fair CRPS (continuous ranked probability score). In the extratropics, the HRES impact is generally neutral while the ENS again shows improvements.

For the extended range, the impact of the physics changes on full-resolution ensemble re-forecasts includes a general increase in spread of a few per cent, particularly in the tropics. Although there are some increases in bias (for example 850 hPa temperature), consistent with the medium range, the impact on bias-corrected scores is approximately neutral (slightly positive in the tropics). The forecast skill of the Madden–

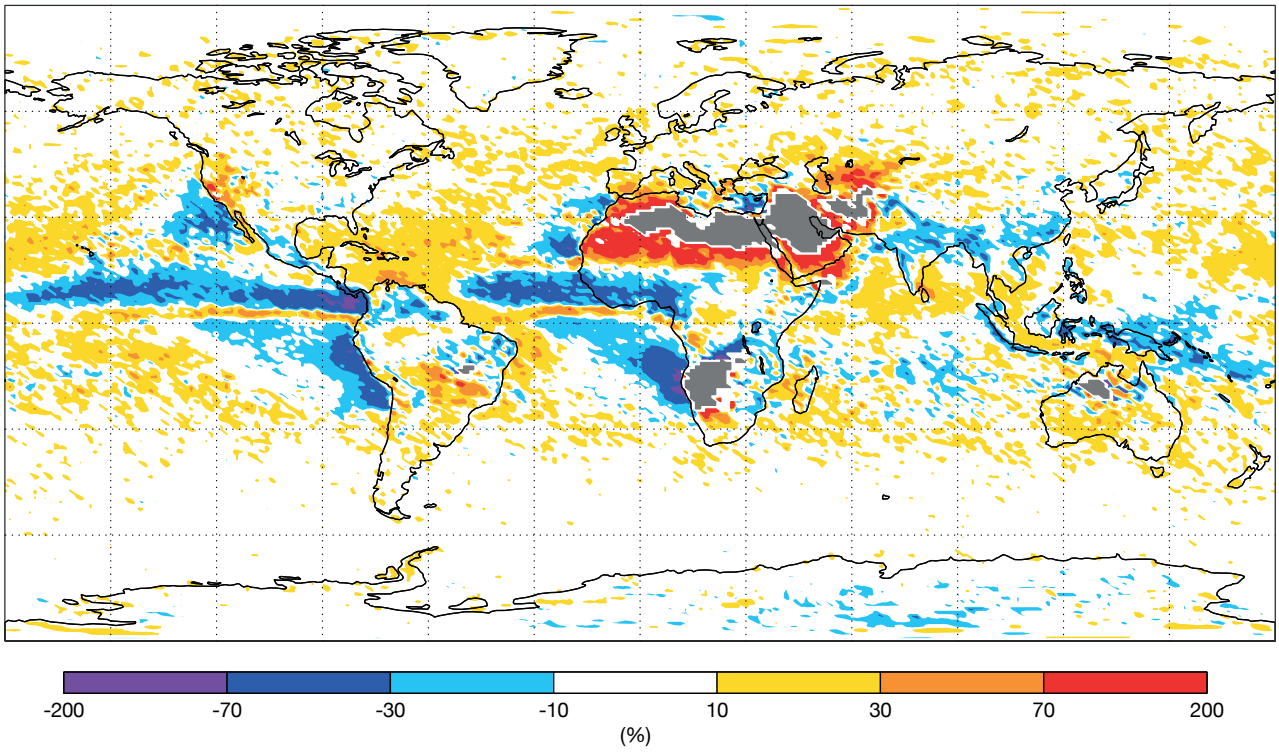

FIGURE 7 Relative difference in the 99th percentile of day-2 precipitation between Cycle 47r3 and Cycle 47r2 model climates from 11-member ensemble re-forecasts over the last 20 years, initialised at 00 UTC on 29 July, highlighting the changes in locally extreme precipitation. Regions where the 99th percentile is zero in both model climates are shaded grey.

Julian Oscillation (MJO) is slightly improved. The overall increase in spread of the MJO index leads to a slight over-dispersion, especially from the 850 hPa zonal wind component of the index. However, the MJO amplitude is increased for lead times greater than five days, reducing amplitude bias (e.g. from –15% to –10% at day 10) and eastward phase bias. There is no significant impact on the frequencies of Euro-Atlantic regimes.

New and revised products

Cycle 47r3 also includes a revision of several forecast products, including an improved calculation of (i) visibility, reducing biases in fog, rain and snow, (ii) wind gusts, reducing an overestimate, (iii) precipitation-type, improving the diagnosis of ice pellets and freezing rain, and (iv) the peak wave period for ocean waves when there are multiple peaks. There are also several new forecast products requested by Member States, including 'MUCAPE' (most-unstable convective available potential energy) now using virtual potential temperature, two new variants of mixed-layer CIN (convective inhibition) and CAPE, and a clear air turbulence (CAT) diagnostic (Bechtold et al., 2021).

Summary

Cycle 47r3 brings a major revision to the representation of moist physics in the IFS as well as improvements in the assimilation of observations and increased usage of satellite data in cloudy regions through the extension of the 'all sky' approach.

An important impact on the forecast is the improvement of the atmospheric circulation, as seen in the increase in skill of extratropical geopotential heights and winds, and with a reduction in wind errors in the tropics of several per cent. The ensemble-mean of error in tropical cyclone position is reduced by 10% between forecast days 2 and 5. There are changes to the character of precipitation, with improvements in the precipitation PDF and in strongly forced convective systems. As well as the many positive signals, a significant change in the physics inevitably leads to some deteriorations, for example in total cloud cover, and these will be addressed in future IFS cycles. There are several new forecast products, such as clear-air turbulence, and improvements to existing products, including visibility and wind gusts.

Overall, the package of changes in Cycle 47r3 is an important step in the development of the IFS, improving performance overall, extending our use of existing observations and providing a stronger foundation for further development of the model and data assimilation at current and higher resolutions.

Further reading

Bechtold, **P.**, **R. Forbes**, **I. Sandu**, **S. Lang** & **M. Ahlgrimm**, 2020: A major moist physics upgrade for the IFS, *ECMWF Newsletter* **No. 164**, 24–32.

Bechtold, **P.**, **M. Bramberger**, **A. Dörnbrack**, **M. Leutbecher** & **L. Isaksen**, 2021: Forecasting clear-air turbulence, *ECMWF Newsletter* **No. 168**, 32–37.

Becker, **T.**, **P. Bechtold** & **I. Sandu**: Characteristics of convective precipitation over tropical Africa in storm-resolving global simulations, *Quarterly Journal of the Royal Meteorological Society*, accepted.

Duncan, **D.**, **N. Bormann**, **A. Geer**, & **P. Weston**, 2021: Assimilation of AMSU-A in all-sky conditions. *EUMETSAT/ ECMWF Fellowship Programme Research Report* **No. 57**.

Lean, **K.** & **N. Bormann**, 2021: Using model cloud information to reassign low level AMVs for NWP. *EUMETSAT/ECMWF Fellowship Programme Research Report* **No. 56**.

Assimilating Spire and COSMIC-2 data into the IFS

Katrin Lonitz, Neill Bowler (UK Met Office), Elias Holm, Sean Healy

During the COVID-19 pandemic in 2020, ECMWF was offered free access to commercial Global Navigation Satellite System Radio Occultation (GNSS-RO) data from Spire Global (Spire in the following). This offer was to partially mitigate the loss of aircraft observations. Without having a chance to test the impact of Spire data in detail, the data was assimilated operationally from 13 May to 30 September 2020, about five weeks after the initial Spire offer. Even before COVID-19 hit the globe, plans were already in the making to perform a detailed investigation of the impact of the assimilation of Spire data into ECMWF's Integrated Forecasting System (IFS) and the UK Met Office system. On 1 July 2020, a project funded by the European Space Agency (ESA) and conducted at ECMWF, the UK Met Office and EUMETSAT started to study exactly this.

The ESA-funded study investigated the impact of assimilating GNSS-RO data from COSMIC-2 and from Spire in both the ECMWF and UK Met Office systems. The project analysed what effect the addition of Spire as well as COSMIC-2 data has by running a series of observing system experiments (OSEs). In addition, ECMWF ran corresponding Ensemble of Data Assimilations (EDA) experiments to investigate the relationship between EDA spread estimates and the OSE short-range forecast error statistics. In particular, these EDA-OSE comparisons enabled us to test previous results obtained with simulated GNSS-RO observations, which suggested that large increases in the GNSS-RO observation numbers would be beneficial. The main finding is that the assimilation of COSMIC-2 and Spire data leads to improvements in medium-range and short-range forecasts. Hence, both ECMWF and the UK Met Office could assimilate Spire data operationally if they were available. We found reasonably good agreement between the EDA spread and the OSE error statistics, suggesting that the EDA technique is a useful method for assessing future observing systems.

What is GNSS-RO?

GNSS-RO is an active satellite measurement technique, where signals from GPS (Global Positioning System) and other GNSS (global navigation satellite systems) are used to retrieve temperature and humidity profile information. Radio occultation (RO) was pioneered in the 1960s. In 1965, the Mariner-4 mission used RO to provide the first measurements of the atmosphere of Mars. The technique is still used by planetary scientists today. The GNSS-RO observations we assimilate at ECMWF use a satellite-to-satellite geometry (see Figure 1). Atmospheric properties like temperature and humidity modify the extent to which the path of the GNSS signal between the satellites is bent. From this bending angle, it is possible to retrieve information about these variables. Measurements using this technique have been assimilated at ECMWF since 2006.

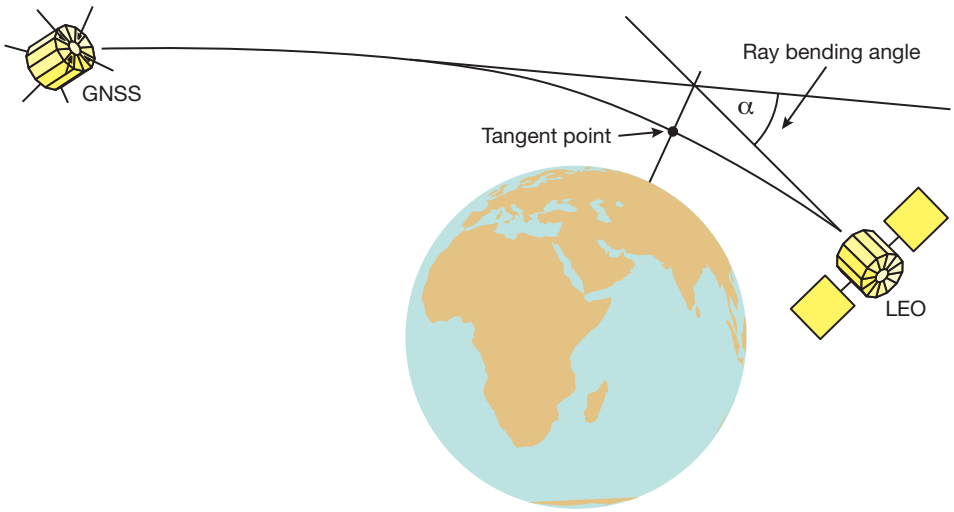

FIGURE 1 A radio signal is emitted by the GNSS satellite and measured with a receiver placed on the low earth orbit (LEO). The path of the radio signal is bent as a result of refractive-index gradients in the atmosphere. The motion of the LEO satellite enables the variation of ray-bending with tangent height to be derived.

doi: 10.21957/kn41xab96l

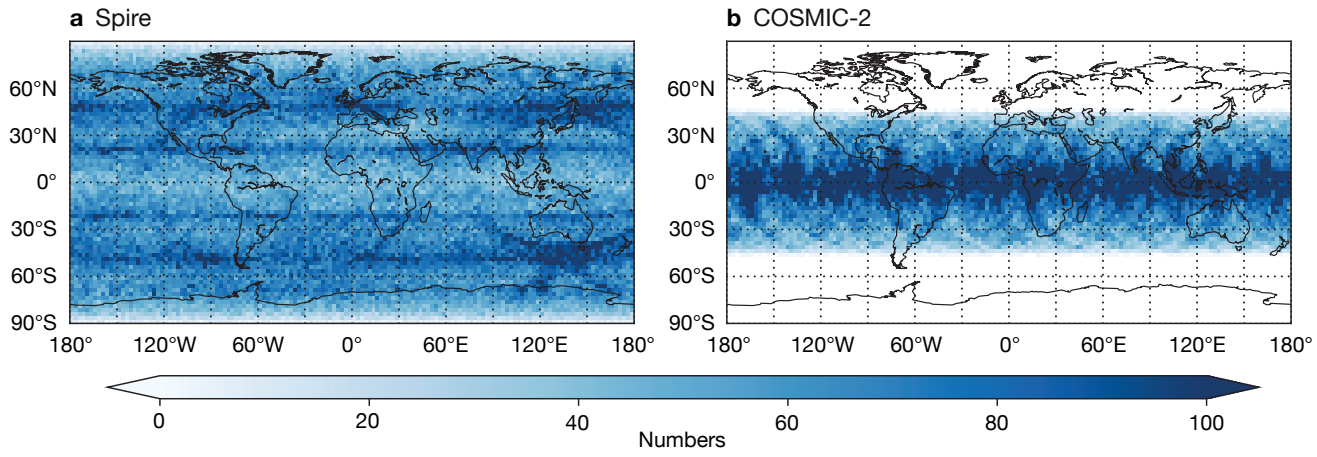

FIGURE 2 Number of occultations for (a) Spire and (b) COSMIC-2 between January and March 2020, regridded to a 2.5 x 2.5 latitude–longitude grid.

Spire and COSMIC-2 data

Spire satellites have a nominal lifetime of 2+ years and new satellites are launched regularly, with updated hardware (Masters et al., 2019). For example, newer satellites have larger solar panels and two occultation antennas allowing the simultaneous collection of both rising and setting occultations. Spire develops the satellites and the GNSS receiver as well as operating a network of 30+ ground stations which provide support, e.g. for data downlinks.

COSMIC-2 (Constellation Observing System for Meteorology, Ionosphere & Climate – 2) is a follow-up mission from COSMIC-1, which was very successful. The cluster of six satellites was launched on 25 June 2019 and spreads along different low-inclination orbits. The main aim of this mission is to perform temperature and humidity soundings as well as making a substantial contribution to space weather applications.

For this study, we received around 5,000 RO profiles from Spire per day globally, and for COSMIC-2 around 4,000 RO profiles per day in a latitude band between ±40 degrees (see Figure 2).

Observing system experiments

Since late 2020, we have run various observing system experiments (OSEs) at ECMWF and the UK Met Office, testing the additional assimilation of Spire and COSMIC-2 (and other GNSS-RO) data into our respective four-dimensional variational (4D-Var) data assimilation systems. The ECMWF experiments use IFS Cycle 47r1 (operational on 30 June 2020), while the UK Met Office uses the setup from parallel suite 43 (operational on 4 December 2019). The experiments ran from 1 January to 31 March 2020, assimilating level-1b bending angle data. The chosen horizontal resolution for the ECMWF experiments is about 25 km (TCo399) and for the UK Met Office experiments about 40 km in the mid-latitudes (N320, 640x480 points on a regular latitude–longitude grid). The experiments are compared to a CONTROL one, which assimilates all observations used operationally for the experimental period. This includes the GNSS-RO data available before COSMIC-2 and Spire.

The experiments carried out in addition to the CONTROL one are:

- **COSMIC2:** This is the CONTROL experiment plus COSMIC-2 data
- **Spire:** This is the CONTROL experiment plus Spire data (only performed by ECMWF)
- **Spire+COSMIC2:** This is the CONTROL experiment plus both Spire and COSMIC-2 data
- **noRO:** This is the CONTROL experiment, but all GNSS-RO has been removed.

Due to numerous differences between the two numerical weather prediction (NWP) systems, we expect to see some differences in the impact of GNSS-RO observations. Some of the principal differences between the NWP systems are:

- The forecasting models are formulated differently. The ECMWF model is based on spherical harmonics, whereas the UK Met Office model uses a finite difference scheme on a regular latitude–longitude grid.
- The resolution of the modelling systems is different, with more than a factor of two in the horizontal resolution.
- There are large differences in the data assimilation systems. The ECMWF system uses a 12-hour assimilation window, whereas the UK Met Office system uses a 6-hour window.

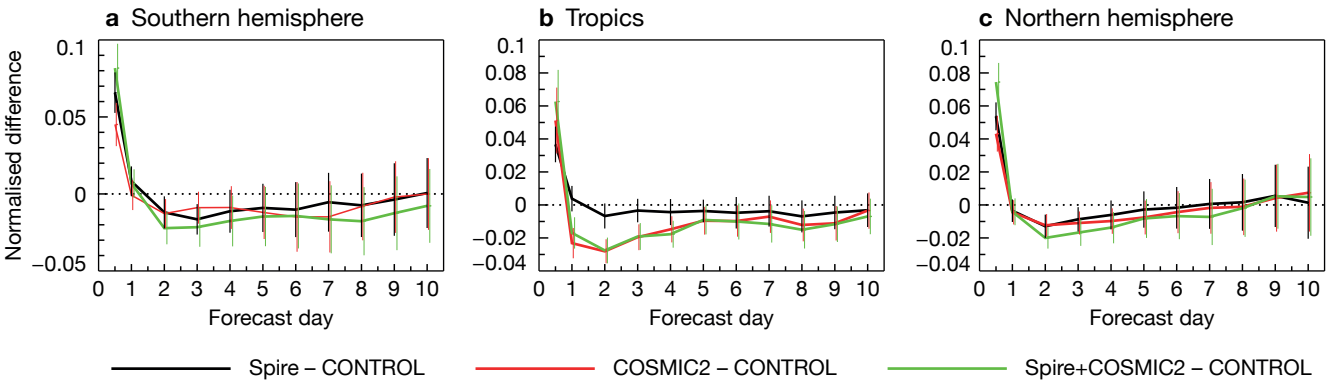

FIGURE 3 Normalised differences in standard deviation in temperature between Spire, COSMIC2 and Spire+COSMIC2 on the one hand, and CONTROL on the other, verified against ECMWF's operational analysis at 100 hPa for different forecast times, for (a) the southern hemisphere (90°S – 20°S); (b) the tropics (20°S – 20°N); and (c) the northern hemisphere (20°N – 90°N). Negative values represent a decrease in standard deviation and positive values an increase in standard deviation. The confidence range is displayed by vertical bars.

- The forward operator used to model bending angles and the weight given to GNSS-RO observations are different (Bowler 2020a).

Results from OSEs

The addition of COSMIC-2 and Spire observations is beneficial in both the ECMWF and UK Met Office systems, with adding Spire on top of COSMIC-2 showing further improvements for some variables and some geographical areas. The largest impact we see from the addition of COSMIC-2 and Spire data can be seen at higher altitudes, which is not surprising as the core region of RO measurements is between heights of 8 km and 30 km. Figure 3 shows how the forecast scores improve with the addition of Spire and COSMIC-2 data compared to CONTROL for temperature at 100 hPa (about 16 km in a standard atmosphere) at ECMWF. Especially in the tropics, the addition of Spire and COSMIC-2 data significantly improves temperature forecast scores between day 1 and 4.

In general, improved medium-range forecast scores and improvement in short-range forecasts can be seen for temperature, humidity and wind, but with different magnitudes in the UK Met Office (not shown) and ECMWF systems. For example, fits to radiosonde temperature observations show improvements of about 5% at 100 hPa when adding Spire and COSMIC-2 for ECMWF in the tropics relative to CONTROL (see Figure 4). Fits to independent observations using the UK Met Office system show generally bigger improvements. For example, in the tropics the addition of Spire and COSMIC-2 show an improvement of about

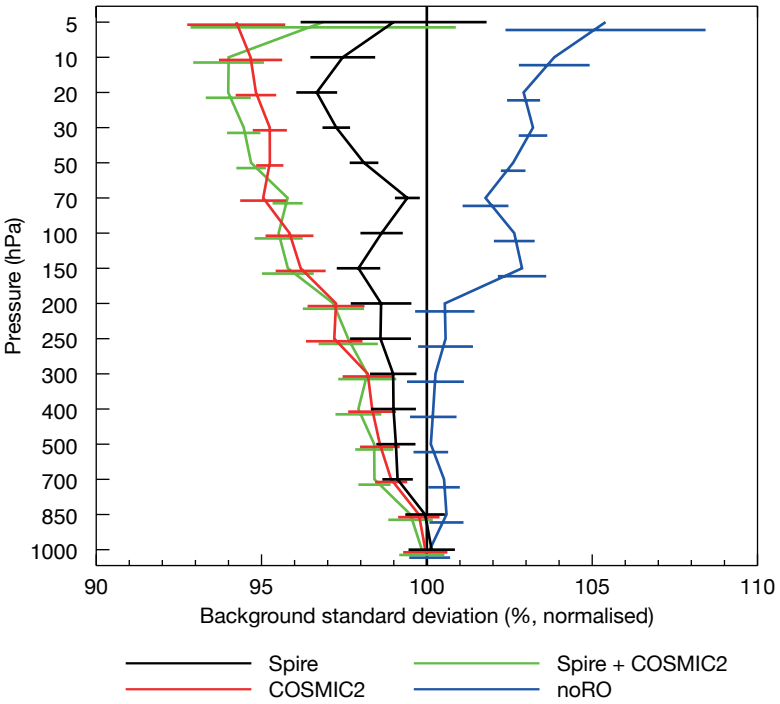

FIGURE 4 Normalised difference in standard deviation of first-guess departures between Spire+COSMIC2 (green), COSMIC2 (red), Spire (black) and noRO (blue) for tropical radiosonde temperature observations at ECMWF. The normalisation is done with respect to the results from CONTROL. Values less than 100% indicate beneficial impacts from the experiments. The horizontal bars indicate the 95% confidence range.

15% for the UK Met Office and 12% for ECMWF compared to noRO in the case mentioned above. The reasons why these differences occur are manifold, but they depend largely on how much skill the assimilation system already has before assimilating additional radio occultation data.

As a result of the addition of Spire and COSMIC-2, ECMWF and the UK Met Office show the largest positive impact in temperature for medium-range forecast scores in the southern hemisphere. For humidity, the biggest impact can be seen with the addition of COSMIC-2 in the tropics at ECMWF, as shown in Figure 5a for the Advanced Technology Microwave Sounder (ATMS) humidity channels 18 to 22. Furthermore, the positive impact for wind when adding Spire and COSMIC-2 could be seen in medium-range forecast scores for both the UK Met Office and ECMWF, with the latter showing this improvement in the short-range, too. For example, the largest improvements in short-range forecast fit to Aeolus data can be seen in the high troposphere and stratosphere (Figure 5b). It is also interesting to note that the additional data by Spire and COSMIC-2 improve the short-range forecast at the same or larger scale as the removal of the other GNSS-RO data degrades it. In fact, the improvements in fits to the humidity-sensitive channels of ATMS are much larger when Spire and COSMIC-2 (Spire, COSMIC2, Spire+COSMIC2) are assimilated than the degradations when GNSS-RO data are removed (noRO). To a lesser extent, the same can also be said for some wind and temperature observations.

Ensemble of Data Assimilations experiments

For ECMWF, we also performed a set of Ensemble of Data Assimilations (EDA) experiments corresponding to the OSEs. The EDA configuration we used in this study consists of ten independent members of 4D-Var data assimilation systems, where observations (including soil moisture), sea-surface temperature, and model physics are perturbed. If those perturbations are correctly specified, the EDA will provide good estimates of analysis and short-range forecast error uncertainties. Harnisch et al. (2013) used the EDA spread values (standard deviation amongst ensemble members) to estimate how the impact of GNSS-RO data scales with the number of observations using simulated GNSS-RO data. More recent work by Bowler (2020b) assimilating Spire data shows some consistency with the Harnisch et al. (2013) scaling plots, but Bowler uses a combined root-mean-square error value averaged over meteorological variables and forecast range, so the quantities are not directly comparable and therefore further investigation is justified. In this study, we have investigated how the relationship between EDA spread and the forecast error statistics changes as the number of real GNSS-RO measurements assimilated increases.

For this reason, we have performed various EDA experiments adding Spire and COSMIC-2 data over about a month, excluding the first nine days because of spin-up. That means the results comprise data from 10 January to 10 February 2020. The following EDA experiments corresponding to the OSEs have been

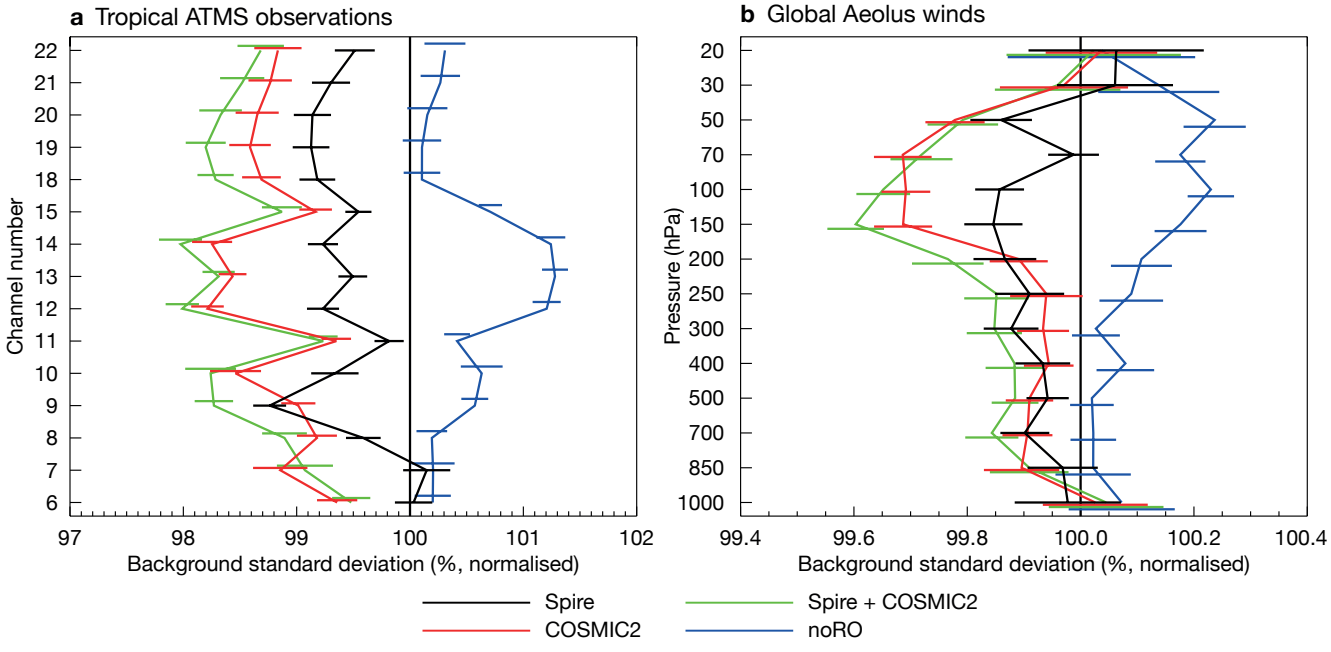

FIGURE 5 Normalised difference in standard deviation of first-guess departures between Spire+COSMIC2 (green), COSMIC2 (red), Spire (black) and noRO (blue) for (a) tropical observations from ATMS and (b) global Aeolus winds. The normalisation is done with results from CONTROL. Values less than 100% indicate beneficial impacts from the experiments. The horizontal bars indicate a 95% confidence range.

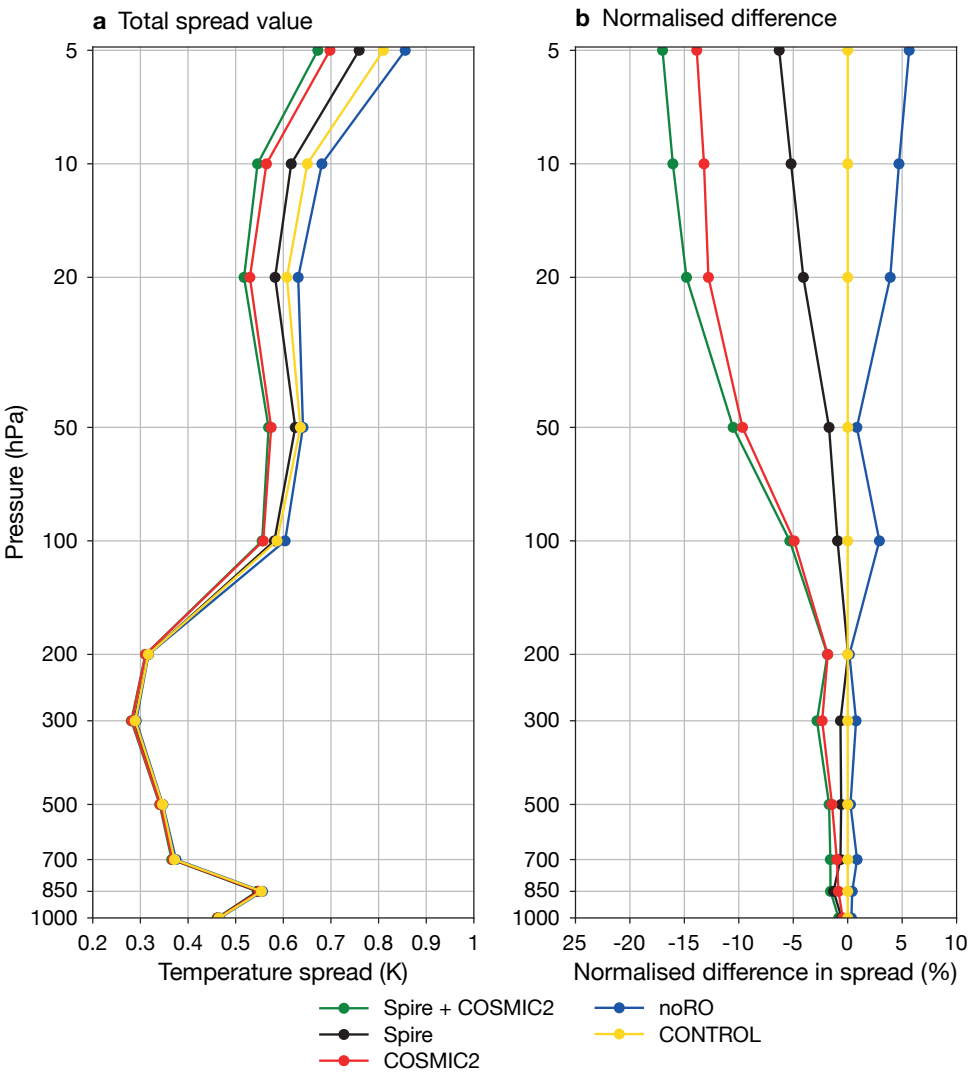

FIGURE 6 Vertical profiles of EDA temperature spread values in the tropics, showing (a) total spread values and (b) total spread values normalised by the CONTROL experiment.

performed: CONTROL, COSMIC2, Spire, Spire+COSMIC2 and noRO. The horizontal model resolution of the EDA experiments is TCo399 using IFS Cycle 47r1 with 137 vertical levels and three inner loops at resolutions of TL95/TL159/TL255. Here we show spread values derived on pressure levels, truncated at spectral wavenumber 255 and gridded onto a reduced Gaussian grid. EDA spread values have been calculated for T+12h.

Results from EDA experiments

The vertical distribution of the EDA spread values for tropical temperature values are shown in Figure 6, with a decrease in EDA spread values with the addition of more GNSS-RO data. In particular, this is true for relatively high levels of 300 hPa (about 9 km) and higher, where the reduction in spread becomes larger with height. For example, at 10 hPa (about 31.5 km) the spread in the tropical temperature values is reduced by about 16% for Spire+COSMIC2 compared to the CONTROL experiment.

How the spread changes for temperature at 10 hPa and 100 hPa can be seen in more detail in Figures 7 and 8, which show the geographical distribution. The largest differences occur in the tropics, where most GNSS-RO is added compared to CONTROL. At 10 hPa, locally more than a 30% reduction in spread can be seen with the addition of Spire and COSMIC-2 data. Already at 100 hPa (see Figure 8), the reduction is more centred along the Intertropical Convergence Zone +/–20° but still reduced significantly by around 10% locally. Here, the larger spread values could be linked to the variability in height of the tropical tropopause layer in the austral summer. These results are in line with Harnisch et al. (2013), showing a systematic decrease in EDA spread values when more GNSS-RO data is added.

The next interesting question is how this decrease in EDA spread scales with the statistics of forecast errors from the corresponding OSEs. To evaluate forecast errors statistics, we use a forecast lead time of 12 hours and verify against the ECMWF operational analysis. Figure 9 shows the vertical distribution of EDA spread values for temperature in the tropics and the corresponding standard deviation of forecast

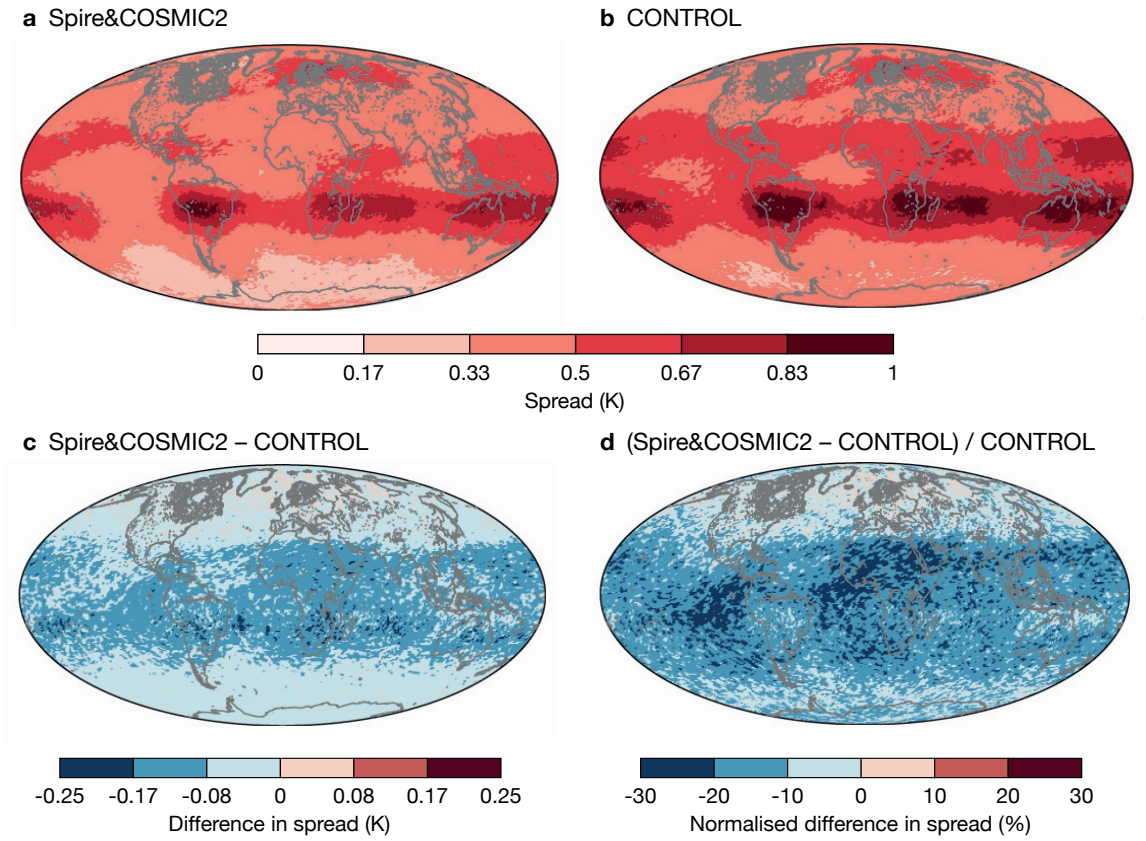

FIGURE 7 Geographical distribution of temperature spread values at 10 hPa for (a) Spire+COSMIC2 (b) CONTROL, (c) the difference between Spire+COSMIC2 and CONTROL, and (d) the normalised difference between Spire+COSMIC2 and CONTROL (normalised by CONTROL).

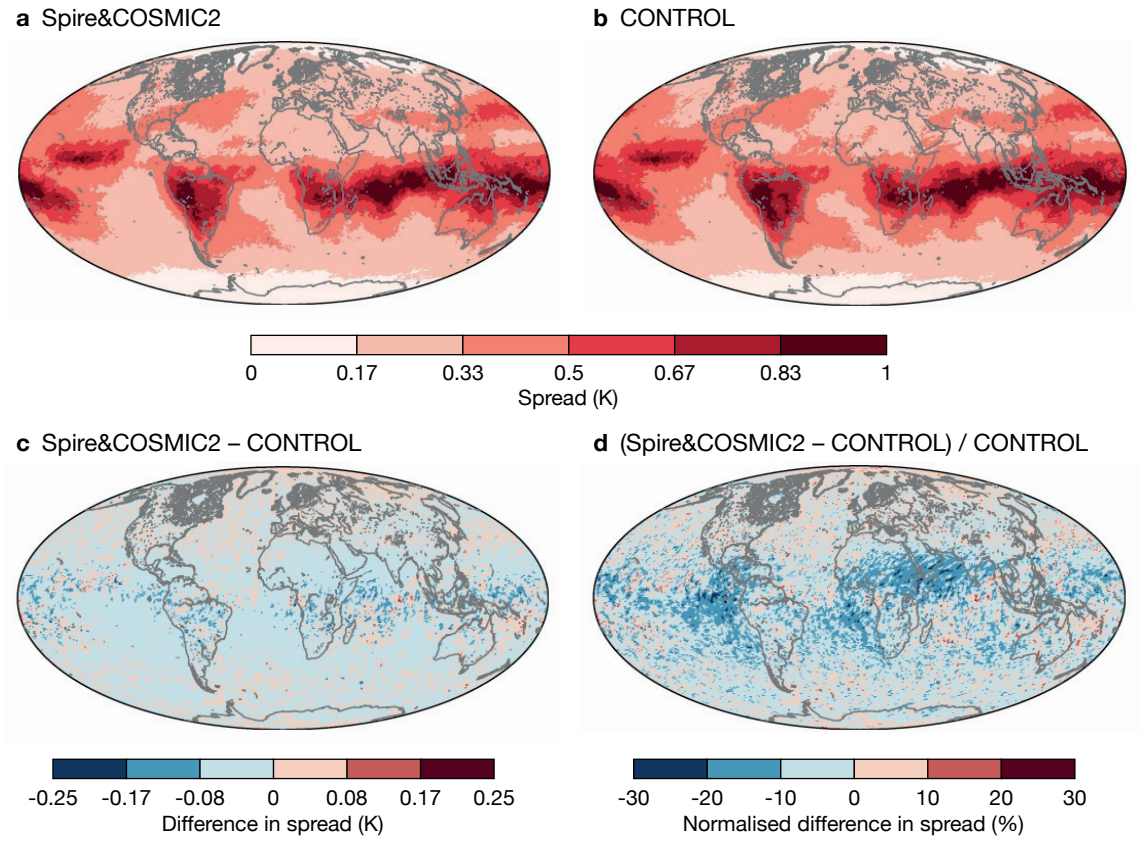

FIGURE 8 The same as Figure 7, but for 100 hPa.

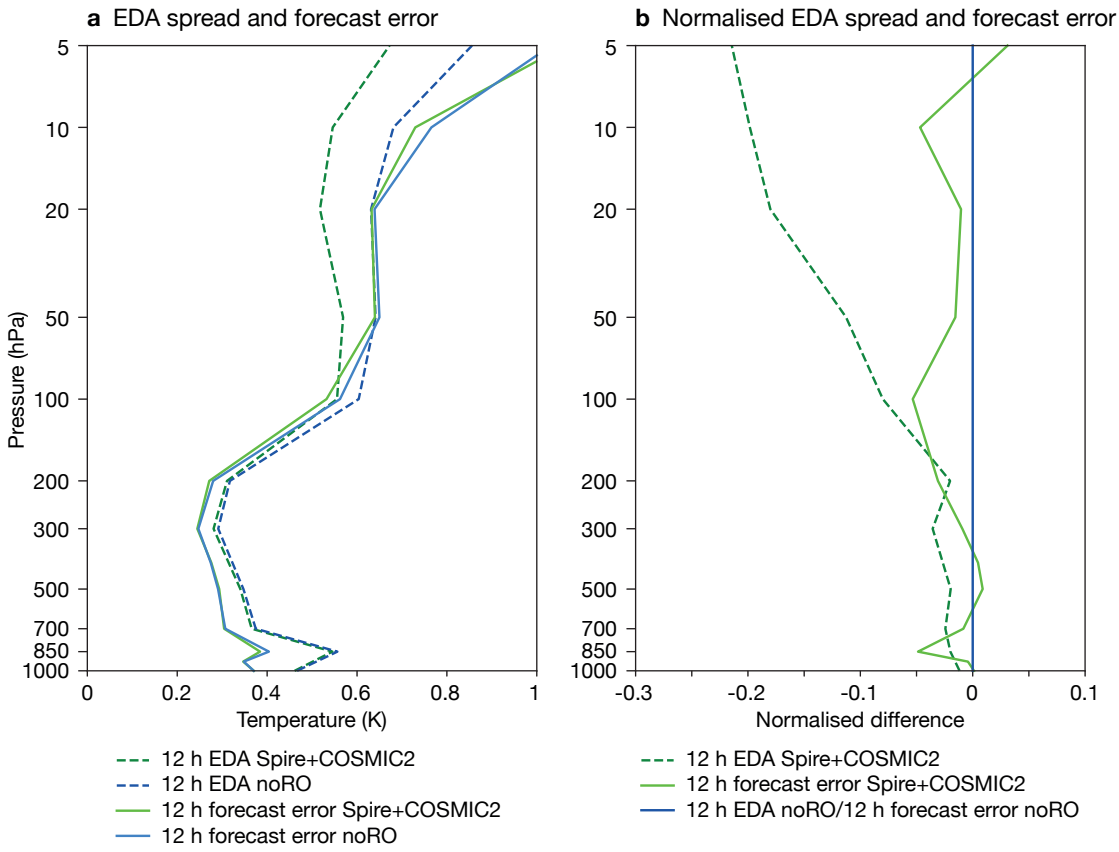

FIGURE 9 Vertical profiles of EDA spread and standard deviation of the forecast error of tropical temperature values for Spire+COSMIC2 and noRO in terms of (a) absolute values and (b) the normalised difference between Spire+COSMIC2 (EDA spread and standard deviation of the forecast error) and noRO (normalised by noRO). Operational analyses are used as a reference for the calculation of the forecast error.

errors for a setup with no GNSS-RO assimilated (noRO) and for Spire+COSMIC2, where all GNSS-RO data are assimilated. In general, the EDA spread in temperature behaves rather similarly to the standard deviation in forecast errors in the troposphere. Larger spread values are seen in the stratosphere (Figure 9a). In relative terms, the spread values and forecast errors decrease for Spire+COSMIC2 compared to noRO (Figure 9b), with a larger decrease for the EDA spread values. One aim of this study is to establish if there is a quantitative relationship between the two measures, as limitations in the EDA experiments and OSEs can have a profound impact on those numbers. In turns out that the relative change in EDA spread values goes in hand with a change in forecast errors when adding GNSS-RO data.

For short forecast lead times, e.g. T+12, the evaluation of forecast errors using analyses can be challenging. Here, the errors in the analysis and forecast can have comparable magnitudes and might be highly correlated (Bormann et al., 2019). This can be compensated by using observations as a reference, instead. For example, we can compare the EDA spread at a given height level with the corresponding departure statistics, using radiosonde data as a reference, for the set of experiments outlined above. The variance of the radiosonde minus forecast departures is the sum of the true forecast error and radiosonde measurement error variances. This suggests the EDA spread, as a measure of forecast error statistics, can be related to first-guess departures with the use of estimates of the radiosonde measurement errors (e.g. Desroziers et al., 2005).

An example of how the variance in first-guess departure statistics scales with the EDA variance when GNSS-RO data is added, for radiosonde temperature measurements at 100 hPa in the tropics, is shown in Figure 10a. Here, a linear relationship between the two measures can be seen, which means that a fixed decrease in EDA spread gives a fixed (but different magnitude) decrease in the variance of first-guess departures from the OSEs. However, this linear relationship cannot be seen in all geographical areas and altitudes. For example, it is not present in the northern hemisphere (Figure 10b). The reason why we see such behaviour is manifold. For example, the distribution of GNSS-RO data (the largest addition of GNSS-RO data is in the tropics), the location and number of radiosonde observations, and maybe the scales included in the shown truncated EDA values could be a reason for this behaviour.

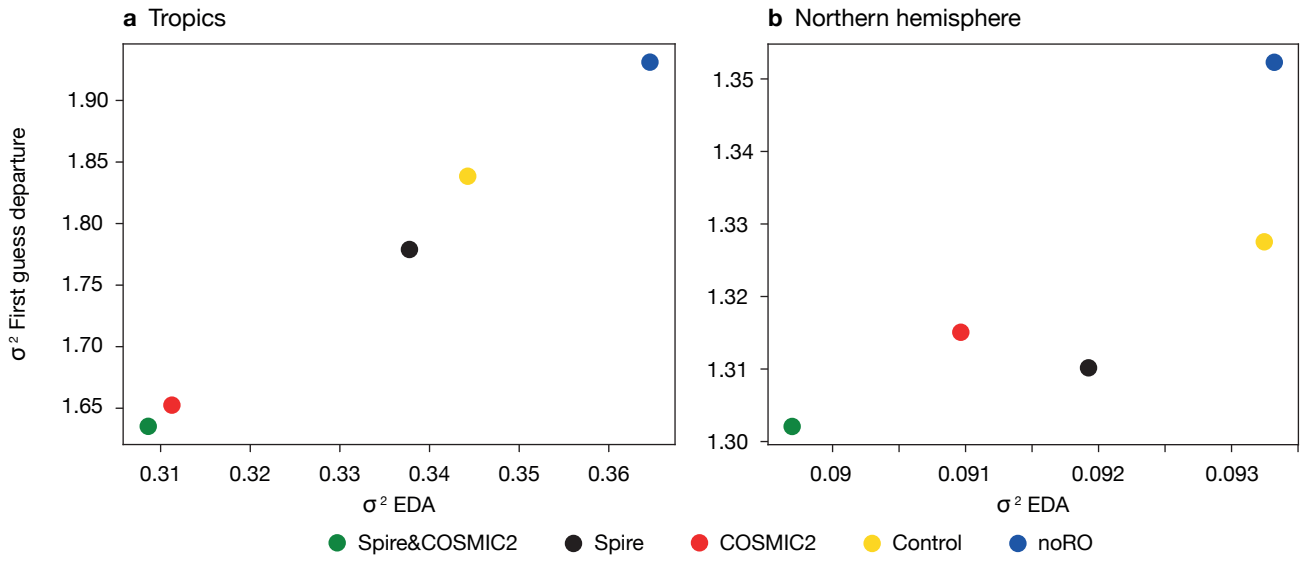

FIGURE 10 Change in variance of first-guess departure using radiosonde temperature measurements from OSEs versus EDA variance in temperature at 100 hPa (a) in the tropics, and (b) in the northern hemisphere.

Summary

In this study we ran different observing system experiments (OSEs) to investigate the impact of supplementary GNSS-RO data. The addition of Spire and COSMIC-2 data has a beneficial impact on forecast scores and fits with independent observations sensitive to humidity, temperature and wind. COSMIC-2 has been operationally assimilated since 25 March 2020, and Spire is planned to be assimilated operationally by early 2022.

Using EDA experiments to estimate the impact of new observations is still a rather new approach. We have tested it with GNSS-RO here, by comparing to results from OSEs. The reductions in EDA spread when adding Spire and COSMIC-2 data are largest in the stratosphere and are qualitatively consistent with reductions in OSE forecast error statistics. Also, results show that this is partially true when EDA statistics are evaluated against radiosonde observations. Hence, we think using EDA spread values is a good approach to assess future observing systems. That being said, none of these measures – EDA spread values, forecast errors from OSEs and fits to observations – are perfect for evaluating the added value obtained from the assimilation of additional GNSS-RO data. Despite their imperfection, one main signal stood out: the continuous addition of a high number of GNSS-RO occultations – Spire and COSMIC-2 data – brings added value to the forecasting system and is far away from reaching saturation point.

Further reading

Bormann, **N.**, **H. Lawrence** & **J. Farnan**, 2019: Global observing system experiments in the ECMWF assimilation system, *ECMWF Technical Memorandum*, **839**.

Bowler, **N.E.**, 2020a: Revised GNSS-RO observation uncertainties in the Met Office NWP system, *Q. J. R. Meteorol. Soc.*, **146**, 2274–2296.

Bowler, **N.E.**, 2020b: An assessment of GNSS radio occultation data produced by Spire, *Q. J. R. Meteorol. Soc.*, **146**, 3772–3788.

Desroziers, **G.**, **L. Berre**, **B. Chapnik** & **P. Poli**, 2005: Diagnosis of observation, background and analysis-error statistics in observation space, *Q. J. R. Meteorol. Soc.*, **131**, 3385–3396.

Harnisch, **F.**, **S.B. Healy**, **P. Bauer** & **S.J. English**, 2013: Scaling of GNSS radio occultation impact with observation number using an ensemble of data assimilations, *Mon. Wea. Rev.*, **141**, 4395–4413.

Healy, **P.**, 2020: ECMWF starts assimilating COSMIC-2 data, *ECMWF Newsletter* **No. 163**, 5–6.

Masters, **D.**, **V. Irisov**, **V. Nguyen**, **T. Duly**, **O. Nogués-Correig**, **L. Tan et al.**, 2019: Status and plans for Spire's growing commercial constellation of GNSS science cubesats, presented at the EUMETSAT ROM SAF-IROWG International Workshop, Helsingør, Denmark, 19–25 September 2019.

Advanced regridding in Metview

Pedro Maciel, Iain Russell

In the last few years, ECMWF's post-processing capabilities have been substantially extended. Part of this success has been the development of the internal interpolation package MIR (Maciel et al., 2017). This is the post-processing engine behind both product generation (pgen) and the client to access the meteorological archive (MARS). Metview, ECMWF's software for accessing, manipulating and visualising meteorological data, has for many years given access to the same post-processing features.

MIR provides sensible defaults, such as interpolation methods and their parametrization, for the roughly 5,000 parameters in the GRIB parameter database (*https://apps.ecmwf.int/codes/grib/param-db*). More recently, developments in Metview have leveraged MIR's more sophisticated regridding functionality. In this article, we shall explore how these features allow users to post-process their parameters of interest beyond the default behaviour for improved results.

Why regrid data?

Why would users want to regrid data? There are many reasons, and users will have their own. The most common is the need to have data from multiple sources, such as datasets and different models or versions of them, in the same geographical representation. Other reasons include reducing the data volume that needs to be transferred or stored, or the need to manipulate the data with specific workflows, for example machine learning. Some workflows will require the data to be stored in a simple regular lat/lon grid, so the output from most numerical weather prediction (NWP) models would need to be regridded in order to be used.

Metview's Regrid module

Metview is an open-source user-facing application developed at ECMWF for exploring and post-processing data related to meteorology. The graphical user interface (GUI) provides a wide range of functionality tailored towards exploring data and developing workflows. Metview's Python interface is open to integration with other applications and communities in many areas, and it can be used in batch, interactive and Jupyter environments. Metview already used the same post-processing engine as the one used in MARS and pgen in its 'Grib Filter' module, but recently the engine was more tightly integrated with Metview for advanced functionality via the new Regrid module. This article focuses on this additional regridding functionality.

Regrid provides Metview with new functionality both in Python and Macro. When run from the GUI, it also has an interactive editor with dynamic properties, designed to encourage exploration. Only a selected few options are initially available, but with a few clicks these options expand, allowing precise specification of how you want your data to be processed (Figure 1).

Interpolation is a very broad topic, and many options that are relatively sophisticated will require further explanation. There are newly introduced methods: a long-awaited conservative method, a series of statistical methods, and finally, advanced k-nearest neighbours interpolation methods. The handling of special values embedded in parameters provided by ECMWF, representing masks and missing values, is also significantly improved and is user controllable. In addition, there is introductory geographic information system (GIS) support.

Choosing an interpolation method

Data has a meaning and is produced with an intent. It is up to the user to know how to use the data, how to explore it and which information is important. It really depends on the application; the solutions are not the same for everyone. In addition, regridding or post-processing in general are destructive procedures.

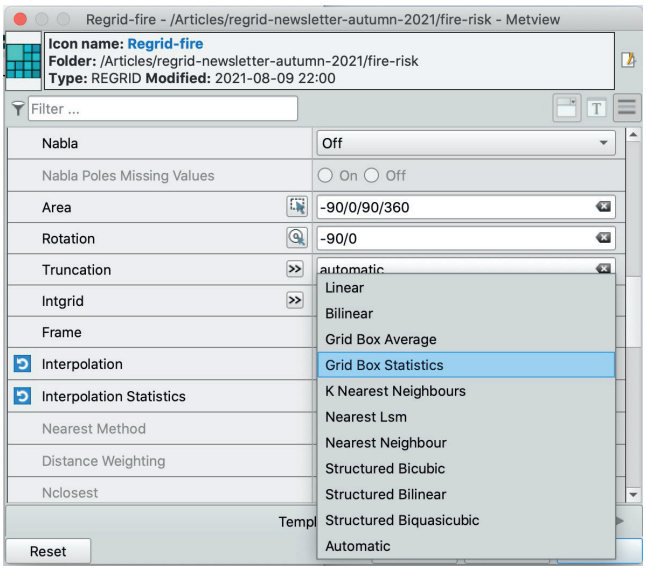

FIGURE 1 The Regrid icon editor in the GUI has many dynamic options.

doi: 10.21957/p77rh351dm

The objective is to preserve most of the signal when processing data. If the field values represent an alert level, then the maximum value in each grid box should likely be preserved. For categorical data, such as vegetation type, consider whether the most common value in a grid box is the one to be preserved. With increasingly large datasets, it helps to be familiar with post-processing techniques in order to extract the most value.

Statistical interpolation

Statistical interpolation is not interpolation in the classical sense, in that the resulting value does not come from a geometrical interpretation of field values, but rather as the statistic of interest from contributing (neighbouring) points.

There are many parameters for which the statistics of interest are maximum, minimum, or mean, such as when handling temperature, alert level, wind gust, precipitation, etc. Other statistics available are count (unlimited or above/below a threshold), standard deviation, variance, skewness, kurtosis, median and mode. Figure 2 shows how the grid-box maximum method preserves high fire danger index values.

Two possible (and available) ways to choose contributing values are the grid-box and Voronoi methods. The grid-box methods simply capture all the source points that lie within a given target grid box. While this is fairly classical and well documented (such as in *https://confluence.ecmwf.int/display/CKB/Model+grid+box+and+time+step*), the Voronoi diagram interpretation is a tessellation defined by a collection of source grid points closest to a target grid point, and thus each polygon of source points does not necessarily cover a regularly shaped area.

Conservative interpolation

The grid box methods interpret a region in space as represented by central points and an associated range in longitude and latitude, up to neighbouring grid boxes. A single grid box is therefore a rectangular region in latitude/longitude centred on a grid point. This is a tessellation comprised of regions of interest around each point, so one can perform statistical interpolation (the grid box statistical interpolation method) similar to the Voronoi statistics method previously described. The grid box interpretation, however, is not extendable to arbitrary sets of points, so it is only currently available for structured, unrotated grids.

Grid boxes are particularly useful for calculating integrals and fluxes when assuming constant values per grid box. This is the basis for grid box conservative interpolation: for one target grid box, which defines its contributions from the area of intersection of the source

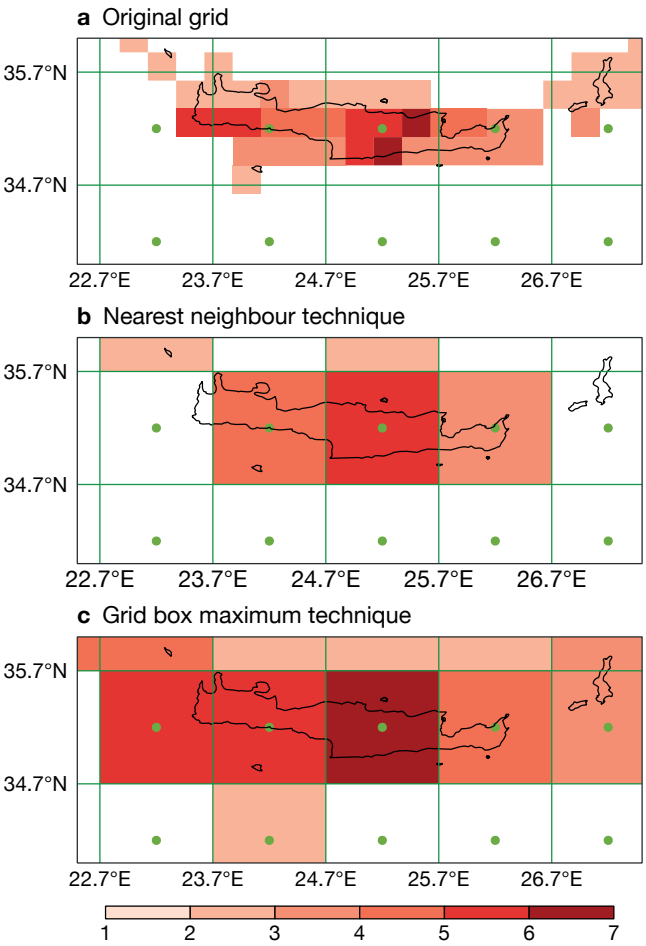

FIGURE 2 Fire danger index data for Crete in the Mediterranean (a) on its original grid, (b) interpolated with the nearest neighbour technique, and (c) interpolated with the grid box maximum technique to preserve the highest warning levels. In all plots, the central points of the target grid boxes are marked in green.

grid boxes, one preserves the integral of the source grid boxes to the target grid box (Figures 3 and 4). This method is not only globally conservative but also locally conservative. It is only up to first-order accurate, but even so it is suitable for many parameters of interest, such as fluxes (ECMWF's Integrated Forecasting System produces many) or integral parameters (such as total column parameters), including precipitation-related parameters, tracers, and aerosols among others. The Copernicus Atmosphere Monitoring Service (CAMS) operated by ECMWF provides a comprehensive list of these types of parameters (*https://atmosphere.copernicus.eu*).

Advanced k-nearest neighbours interpolation

In some cases, the representation of points in space is better interpreted without structure (a disjoint cloud of points). In that case, the source values contributing to a target point depend on how far away they are. The k-nearest neighbours interpolation controls

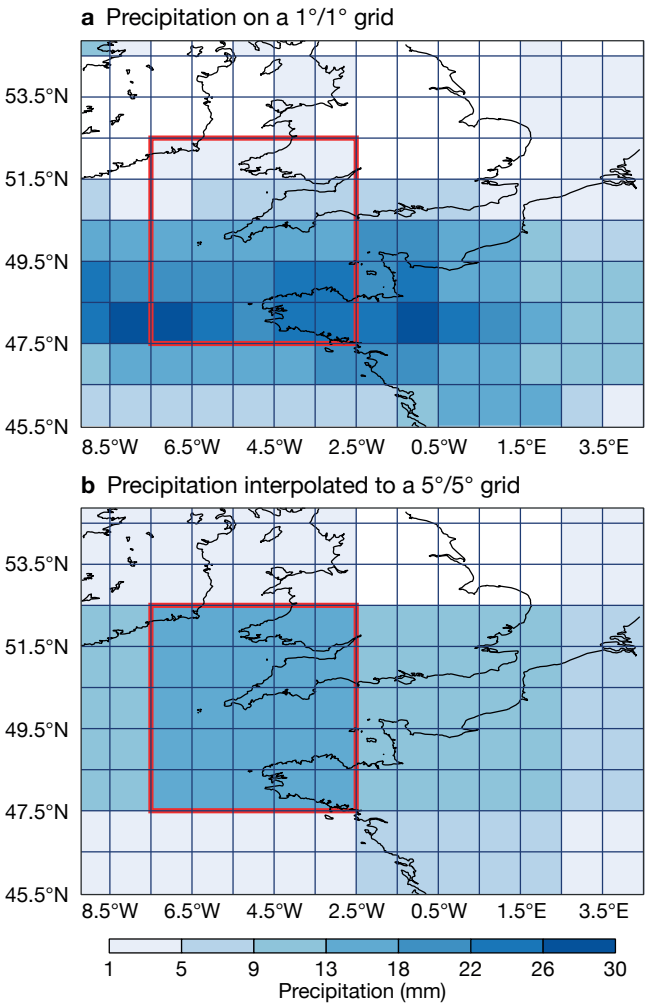

FIGURE 3 Precipitation over six hours in southern Britain and northern France (a) on its original 1°/1° grid, and (b) interpolated to a 5°/5° grid using the grid box average technique. The value of each resulting grid box, such as the one highlighted in red, is the spatially-weighted average of the source grid boxes that cover its area, meaning that total quantities are conserved within each grid box and over the entire data.

two aspects: how the source points are selected (relative to a target point) by distance or number, and how these selected points are weighted (calculation of their contribution).

Distinct ways of selecting the source points are:

- by number (k), irrespective of distance
- by distance/radius, irrespective of number
- by number and up to a distance (intersection of sets by number and distance)
- by number or up to a distance (union of sets), and
- by sampling points selected by distance.

To control how the selected points contribute, one common method is inverse distance weighting (IDW) with contributions calculated as a weighted average

```
import metview as mv

precip = mv.read('precip.grib')

gbavg = mv.regrid(
    grid = [5,5],
    area = [40, -20, 60, 20],
    interpolation = "grid_box_average",
    data = precip)
```

FIGURE 4 Python code to regrid precipitation GRIB data using the conservative grid box average method to produce data on a 5°/5° grid on a subarea.

based on distance (more distance assigns less weight). The Shepard method is the general case of this: it defines IDW, IDW squared, and IDW to a user-specified power. Another type is distance-free weighting, which is just straightforward averaging. It does not employ distance and therefore is relevant where different resolutions are used for the same workflow, suitable for machine learning applications training at lower resolution and application at higher resolution. And finally, special options exist distributing weighting according to distance over a Gaussian curve (user-defined by standard deviation, centred on each target point), or for specific purposes such as handling topographic data at model resolution – a smoothing operator. The following options are available:

- inverse distance weighting (including the Shepard method)
- distance weighting following Gaussian function curve
- no distance weighting (resolution independent)
- orography climate filter smoothing (see *https://www.ecmwf.int/en/publications/ifs-documentation*, CY47r1 - Part IV: Physical Processes).

Handling of missing and special values

Several parameters might not be completely defined over the whole globe or are only defined over some specific areas. This is the case for many surface parameters, which have values only defined over land or sea. Values over other areas are routinely referred to as missing, and the handling of missing values is generally transparent to the user: they are not included when interpolating.

Points representing missing values are never involved in interpolation, and the remaining contributions are always linearly re-weighted (to sum to one). Regrid allows finer control over this handling: an output value can be set to missing if all, any or the heaviest-weighted (according to the interpolation method) of its contributing points are missing.

The control over this behaviour has a strong effect, for example, on the way land-defined values are represented over the sea on interpolation, or vice-versa. This specifically affects values near coastlines. The missing-if-any-is-missing favours missing values, missing-if-all-are-missing favours non-missing values, and missing-if-heaviest-is-missing is in between (the default behaviour). The default behaviour works better than the others across large resolution changes.

Some parameters include values that have a semantic rather than physical meaning. These include the missing values mentioned above, but also other specific values, depending how the data is intended to be interpreted. For example, sea-surface temperature (°C) has a value of 0 over land, for some products representing the absence of data, or snow depth (m) has a value of 10, representing a glacier.

These values should not interfere with the interpolation of physically relevant values. Regrid offers a mechanism to control these, by specifying a value and tolerance to compare with. This user-defined tolerance addresses a practical concern, as field values might be encoded approximately, not exactly, to the original value, especially when archived (in MARS) or stored on disk in GRIB or netCDF formats.

GIS applications

For applications where a precise description of location is required, for example because of information exchange with other data sources or producers, Regrid has support for PROJ-based projections. This well-known library handles all kinds of cartographic projections and supports several spatial analysis applications. It is ideal for handling data from local area models with very specific projections.

PROJ support at ECMWF starts with the ecCodes ability to generate a PROJ string to describe a coordinate reference system (CRS) from GRIB-encoded data. MARS hosts a great variety of data, including many LAM model grids on a variety of projections, e.g. Lambert conformal conic (LCC), Lambert azimuthal equal-area (LAEA) and Mercator.

Regrid supports this kind of GRIB format GIS-compliant data as input, and in addition it supports built-in mappings from either PROJ strings or EPSG codes (a short, concise way to specify a CRS) to GRIB output. The assignment of CRS to specific grids needs to be agreed with data producers in advance.

As an application example, the European Flood Awareness System (EFAS) operates on a European scale to provide coherent medium-range flood forecasts, implemented by ECMWF. The EFAS workflow is supported with an LAEA grid specified with a particular EPSG code, and its products are integrated in a variety of GIS workflows. With this added support, Regrid results are well integrated either as a source to, or target from, EFAS products.

Using templates

A common task is to put GRIB file ‘A’ onto the same grid as GRIB file ‘B’. Regrid can simplify this process by allowing the use of a template GRIB. Instead of supplying the various parameters required to reproduce the target grid, the user can provide a sample GRIB file, and its grid parameters will be read and used to generate the output (Figure 5).

```
import metview as mv

data = mv.read("global_1_deg.grib")

new_data = mv.regrid(
    data = data,
    interpolation = "nearest_neighbour",
    grid_definition_mode = "template",
    template_source = "/path/to/subarea_3_deg.grib")

new_data.write("regridded_data.grib")
```

FIGURE 5 Python code to regrid one GRIB file using another as a template.

Availability

Metview is installed on ECMWF’s computing platforms including the Member and Co-operating State server ECGATE. For use external to ECMWF’s computing platforms, Metview is also available as a binary installation on the conda platform, available through the conda-forge channel with one of these commands:

```
conda install metview -c conda-forge
conda install metview-batch -c conda-forge
# no GUI installed
```

The Python interface can be installed with either of these commands:

```
conda install metview-python -c conda-forge
pip install metview
```

Metview’s Python documentation has been moved to readthedocs and can be accessed here: *https://metview.readthedocs.io/en/latest/*. A Jupyter notebook containing the examples described in this article can also be found there.

Further reading

Maciel, **P.**, **T. Quintino**, **U. Modigliani**, **P. Dando**, **B. Raoult**, **W. Deconninck et al.**, 2017: The new ECMWF interpolation package MIR, *ECMWF Newsletter* **No. 152**, 36–39.

ECMWF publications

(see *www.ecmwf.int/en/research/publications*)

Technical Memoranda

887 **Williams**, **R.**, **R. Hogan**, **I. Polichtchouk**, **M. Hegglin**, **T. Stockdale** & **J. Flemming**: Evaluating the impact of prognostic ozone in IFS NWP forecasts. *October 2021*

886 **N. Bormann**: Investigating the use of Lambertian reflection in the assimilation of surface-sensitive microwave sounding radiances over snow and sea-ice. *September 2021*

885 **T. Hewson**: Use and Verification of ECMWF products in Member and Co-operating States. *September 2021*

884 **T. Haiden**, **M. Janousek**, **F. Vitart**, **Z. Ben-Bouallegue**, **L. Ferranti** & **F. Prates**: Evaluation of ECMWF forecasts, including the 2021 upgrade. *September 2021*

ESA Contract Reports

Weston, **P.** & **P. de Rosnay**: Quarter 2 2021: Operations Service Report. *July 2021*

Weston, **P.**, **P. de Rosnay** & **S. English**: GRDS test-bed report. *May 2021*

Weston, **P.** & **P. de Rosnay**: Quarter 1 2021: Operations Service Report. *April 2021*

EUMETSAT/ECMWF Fellowship Programme Research Reports

57 **Duncan**, **D.**, **N. Bormann**, **A.J. Geer** & **P. Weston**: Assimilation of AMSU-A in All-sky Conditions. *October 2021*

ECMWF Calendar 2021/22

2021	
Nov 4	Extraordinary session of Council
Nov 10–11	European Weather Cloud User Workshop
Nov 15–18	ESA–ECMWF workshop on machine learning for Earth system observation and prediction
Dec 2–3	Council
2022	
Feb 7–10	Training course: Use and interpretation of ECMWF products
Feb 14–18	Radio Frequency Interference 2022 workshop
Feb 28–Mar 4	Training course: Data assimilation
Mar 7–11	Training course: Satellite data assimilation
Mar 21–25	Training course: Predictability
Mar 28–Apr 1	Training course: Parametrization
Apr 12	Advisory Committee for Data Policy (Darmstadt)
Apr 25–29	Training course: Advanced numerical methods for Earth system modelling
Apr 26–27	Finance Committee
Apr 27	Policy Advisory Committee
May 3–6	Training course: Machine learning for weather prediction
May 9–12	Workshop on model uncertainty
May 16–20	Training course: A hands-on introduction to NWP models
Jun 7–10	Using ECMWF's forecasts (UEF2022)
Jun 13–17	Online Computing Week
Jun 28–29	Council
Sep 12–16	Annual Seminar 2022
Oct 3–5	Scientific Advisory Committee
Oct 3–6	Training course: Use and interpretation of ECMWF products
Oct 6	Advisory Committee of Co-operating States
Oct 6–7	Technical Advisory Committee
Oct 20–21	Finance Committee
Oct 21	Policy Advisory Committee
Oct 31–Nov 4	Sixth WGNE workshop on systematic errors in weather and climate models
Dec 1–2	Council

Contact information

ECMWF, Shinfield Park, Reading, RG2 9AX, UK

Telephone National 0118 949 9000

Telephone International +44 118 949 9000

Fax +44 118 986 9450

ECMWF's public website *www.ecmwf.int/*

E-mail: The e-mail address of an individual at the Centre is firstinitial.lastname@ecmwf.int. For double-barrelled names use a hyphen (e.g. j-n.name-name@ecmwf.int).

For any query, issue or feedback, please contact ECMWF's Service Desk at *servicedesk@ecmwf.int*.

Please specify whether your query is related to forecast products, computing and archiving services, the installation of a software package, access to ECMWF data, or any other issue. The more precise you are, the more quickly we will be able to deal with your query.

ECMWF

Newsletter | **No. 169** | Autumn 2021

European Centre for Medium-Range Weather Forecasts

www.ecmwf.int